

# Classical and quantum dimers on the star lattice

John Ove Fjærestad<sup>1</sup>

<sup>1</sup>*Department of Physics, The University of Queensland, Brisbane, QLD 4072, Australia*

(Dated: November 24, 2008)

We consider dimers on the star lattice (aka the 3-12, Fisher, expanded kagome or triangle-honeycomb lattice). We show that dimer coverings on this lattice have  $Z_2$  arrow and pseudo-spin representations analogous to those for the kagome lattice, and use these to construct an exactly solvable quantum dimer model (QDM) with a Rokhsar-Kivelson (RK) ground state. This QDM, first discussed by Moessner and Sondhi from a different point of view, is the star-lattice analogue of a kagome-lattice QDM analyzed by Misguich *et al.* We give a detailed analysis of various properties of the classical equal-weight dimer model on the star lattice, most of which are related to those of the RK state. Using both the arrow representation and the fermionic path integral formulation of the Pfaffian method, we calculate the number of dimer coverings, dimer occupation probabilities, and dimer, vison, and monomer correlation functions. We show that a dimer is uncorrelated with dimers further away than on neighboring triangles, that the vison-vison correlation function vanishes, and that the monomer-monomer correlation function equals  $1/4$  regardless of the monomer positions (with one exception). A key result in the fermionic approach is the vanishing of the two-point Green function beyond a short distance. These properties are very similar to those of dimers on the kagome lattice. We also discuss some generalizations involving arrow representations for dimer coverings on “general Fisher lattices” and their “reduced” lattices, with the kagome, squagome, and triangular kagome lattice being examples of the latter.

PACS numbers: 71.10.-w, 74.20.Mn, 05.50.+q

## I. INTRODUCTION

Classical dimer models (CDMs) have long been of interest in statistical and theoretical physics.<sup>1,2,3,4,5</sup> An important breakthrough was ushered in with the solution of the dimer problem on the square lattice in terms of Pfaffians.<sup>6,7,8</sup> In a subsequent seminal paper,<sup>9</sup> Kasteleyn generalized this solution method to the dimer problem on any planar lattice, and also showed explicitly that CDMs can exhibit singularities, corresponding to phase transitions, as a function of the dimer weights. A few years later Fisher showed that the Ising model on an arbitrary planar lattice can be mapped to a CDM on a different planar lattice,<sup>10</sup> thus making it possible to solve the former class of models with the Pfaffian method developed for the latter. More recently, Moessner and Sondhi<sup>11</sup> have demonstrated that the nature of the phases and phase transitions in the two models connected by this mapping can be very different. Specifically, they revisited Fisher’s mapping between the ferromagnetic Ising model on the square lattice and the CDM on the star lattice<sup>12</sup> (shown in Fig. 1) and found that the symmetry-breaking transition in the former model maps to a confinement-deconfinement transition for test monomers in the latter.

Over the last two decades, quantum dimer models (QDMs) have come to play an important role in the search for phases with exotic types of orders and excitations in quantum antiferromagnets (for recent reviews, see Refs. 13 and 14). Most intriguingly, there is the possibility of spin liquid phases<sup>15</sup> with deconfined, fractionalized (spin- $1/2$  *spinon*) excitations. These spin liquids do not break spin rotation or spatial symmetries but are instead characterized by unconventional *quantum orders*<sup>16</sup>

(e.g. topological order) not describable by local order parameters. The canonical example of a spin liquid is a short-range resonating-valence-bond (RVB) state<sup>15</sup> given by a macroscopic superposition of products of spin singlets formed by pairs of nearest-neighbor spins. QDMs were introduced by Rokhsar and Kivelson<sup>17</sup> to be an approximate, effective description of the low-energy physics when it is dominated by such short-range singlet fluctuations.

The set of dimer coverings in a CDM is taken to form an orthogonal basis for the Hilbert space of QDMs on the same lattice. A QDM Hamiltonian can contain both potential and kinetic energy terms, which are respectively diagonal and off-diagonal in this dimer basis. If these terms have amplitudes  $v$  and  $t$  respectively, the QDM ground state will be a function of  $v/t$ . This parameter space generally includes a so-called Rokhsar-Kivelson (RK) point, at which the ground state is an equal-amplitude superposition of dimer coverings (in each topological sector).<sup>17</sup> As a consequence, there is a close relationship between QDMs at the RK point and CDMs: any ground state correlation function at the RK point that only involves operators which are diagonal in the dimer basis (e.g., the dimer-dimer or vison-vison correlation function) is equal to the corresponding correlation function for the CDM with equal dimer weights on the same lattice.<sup>17</sup>

The search for dimer liquids in QDMs was crowned with success when Moessner and Sondhi<sup>18</sup> showed that the ground state of the triangular-lattice QDM is a dimer liquid (i.e. has exponentially decaying dimer-dimer correlations) over a finite range of  $v/t$ . In another remarkable paper, Misguich *et al.*<sup>19</sup> introduced and analyzed a

QDM on the kagome lattice that differed in several respects from the QDMs studied until then. This kagome QDM does not have potential energy terms, and its kinetic energy involves flippable loops<sup>20</sup> of various lengths (in contrast, the prototypical QDM studied in Refs. 17 and 18 only includes the shortest flippable loops). Due to special properties of the kagome lattice, which allow for  $Z_2$  arrow and pseudo-spin representations of its dimer coverings,<sup>19,21,22</sup> Misguich *et al.*<sup>19</sup> were able to show that this QDM can be written in an extremely simple form in terms of the pseudo-spin variables. As a consequence, all its eigenstates and eigenvalues are exactly known. In particular, its ground state in each topological sector is the RK (equal-amplitude) state. On the kagome lattice this state is an extremely disordered dimer liquid: the dimer-dimer correlations vanish for dimers further apart than on neighboring triangles. This has been shown from the arrow representation<sup>19</sup> as well as from Pfaffian calculations of the dimer-dimer correlations of the CDM on the kagome lattice.<sup>23,24</sup> Another interesting result for the CDM on the kagome lattice is related to monomer deconfinement: the monomer-monomer correlation function equals 1/4 regardless of the distance between the two monomers. Again, this has been shown both from the arrow representation<sup>25</sup> and from Pfaffian calculations.<sup>26</sup>

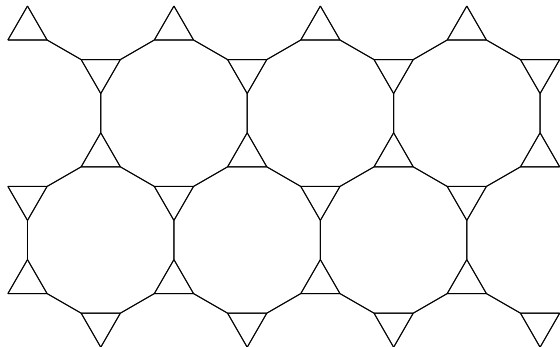


FIG. 1: The star lattice. The lattice sites are the vertices in this figure. The lines connecting the sites will be called bonds. There are two types of bonds, which will be referred to as triangle bonds and linking bonds. A triangle bond is part of a triangle. A linking bond connects two neighboring triangles.

In this paper we consider dimers on the star lattice<sup>12</sup> (Fig. 1), a non-bipartite lattice that is one of the 11 Archimedean tilings.<sup>27</sup> Because of its frustration<sup>28</sup> and small coordination number ( $z = 3$ ) this is an interesting lattice to consider in the search for unconventional phases in spin and dimer models. Various studies of this kind have recently appeared in the literature. We have already mentioned Ref. 11 which we will come back to shortly. From an analysis of exact diagonalization spectra Richter *et al.*<sup>28</sup> concluded that the kagome and star lattices are the only Archimedean tilings for which the ground state of the nearest-neighbor spin-1/2 Heisen-

berg model does not have magnetic long-range order. For the star lattice the ground state is instead a unique valence bond crystal (VBC) with singlets across the bonds that link different triangles.<sup>28,29</sup> If the exchange across these linking bonds is made sufficiently small compared to that of the triangle bonds, exact diagonalization results suggest that the ground state is a different, three-fold degenerate VBC.<sup>30</sup> We also note that an experimental realization of a star antiferromagnet,  $[\text{Fe}_3(\mu_3\text{-O})(\mu\text{-OAc})_6\text{-}(\text{H}_2\text{O})_3][\text{Fe}_3(\mu_3\text{-O})(\mu\text{-OAc})_{7.5}]_2 \cdot 7\text{H}_2\text{O}$ , has been reported recently.<sup>31</sup> Furthermore, Yao and Kivelson<sup>32</sup> have shown that the ground state of the Kitaev model on the star lattice is a chiral spin liquid.

We show that dimers on the star lattice have properties that are very similar to those for the kagome lattice summarized above. We first show that dimer coverings on the star lattice have arrow and pseudo-spin representations analogous to those for the kagome lattice. We use these to construct a star-lattice QDM that has similar properties as the kagome QDM discussed by Misguich *et al.*<sup>19</sup> In particular, its ground state is the RK state. This star-lattice QDM was first discussed in Ref. 11 as a special case of a QDM introduced there via a modified Fisher construction mapping it to a three-dimensional Ising model in the time-continuum limit. We give a detailed analysis of the star-lattice CDM for equal-weight dimers (the case related to the RK ground state as mentioned above), using both the Pfaffian method and the arrow representation to calculate the number of dimer coverings (on a finite lattice without boundaries), dimer occupation probabilities, and dimer, vison, and monomer correlation functions.

For our Pfaffian calculations we use Samuel’s formulation based on a path integral description of free Majorana fermions.<sup>33</sup> We find that the (two-point) Green function of the fermions vanishes beyond a short distance. This is a key result that causes a dimer to be uncorrelated with all dimers further away than on a neighboring triangle. It furthermore makes the calculations of the vison-vison and monomer-monomer correlation functions tractable; although in the fermionic formulation these functions contain a “string” going from one vison/monomer to the other, which makes the number of pairings from Wick’s theorem grow exponentially with the vison/monomer separation, the number of *nonzero* pairings is strongly reduced by the above property of the Green function. We also use the arrow representation to calculate the various quantities considered. These arrow derivations are conceptually simpler and more intuitive than the Pfaffian ones, in part because they lend themselves to a pictorial representation. Finally, we consider some generalizations to general Fisher lattices (any lattice hosting the dimers in Fisher’s mapping<sup>10</sup>), and discuss “reduced” lattices of these (examples of which include the kagome, squagome, and triangular kagome lattice).

The paper is organized as follows. The arrow and pseudo-spin representation are introduced in Secs. II and

III. In Sec. III we also construct the exactly solvable QDM. The number of dimer coverings is considered in Sec. IV. The Green function is calculated in Sec. V. In Secs. VI and VII we discuss dimer occupation probabilities and dimer correlations. The vison-vison and monomer-monomer correlation functions are calculated in Secs. VIII and IX. In Sec. X we summarize similarities and connections between dimers on the star and kagome lattice. In Sec. XI we discuss properties of general Fisher lattices and their reduced lattices (with some technical details relegated to Appendix B). Some concluding remarks are given in Sec. XII. In Appendix A we present an alternative pseudo-spin representation of dimer coverings on the star lattice.

## II. ARROW REPRESENTATION OF DIMER COVERINGS

In this section we show that there is a one-to-one correspondence between dimer coverings and arrow configurations on the star lattice. The arrows are Ising degrees of freedom located on the lattice sites. First, however, we establish some basic terminology that will be used throughout the paper.

The star lattice consists of triangles and dodecagons as shown in Fig. 1. The lattice sites sit at the vertices of the polygons. The thin lines connecting different sites will be referred to as bonds. While all sites in the star lattice have the same local environment (by definition of an Archimedean tiling), there are two types of inequivalent bonds, which will be referred to as triangle bonds and linking bonds. A triangle bond is part of a triangle (as well as a dodecagon) while a linking bond is part of two dodecagons and is a link between two triangles.

A bond can be occupied by a dimer, which will be drawn as a thicker line on the bond. The dimer touches the two sites that are connected by the bond. We will consider close-packed, hard-core dimer configurations. Close-packed means that no site is left untouched by a dimer. Hard-core means that no site is touched by more than one dimer. The fact that each site is touched by exactly one dimer will be referred to as the closed-packed, hard-core constraint. In the following we will refer to such dimer configurations simply as dimer coverings. (In Sec. IX we will relax the close-packed part of the constraint to consider dimer-monomer configurations in which two sites in the lattice are not touched by a dimer.) An example of a dimer covering on the star lattice is shown in Fig. 2(top).

Elser and Zeng showed that dimer coverings on the kagome lattice allow for an arrow representation.<sup>21</sup> Misguich *et al.* made extensive use of this representation in their work on QDMs on the kagome lattice,<sup>19,22</sup> and also pointed out that the arrow representation can be generalized further to all lattices made of corner-sharing triangles. We will now show that an arrow representation exists for dimer coverings on the star lattice too (arrow

representations for some other lattices will be discussed in Sec. XI and XII).

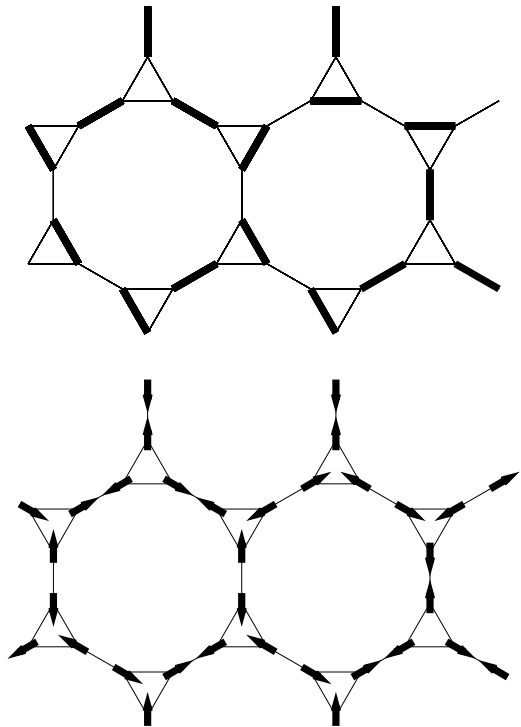


FIG. 2: Top: Example of dimer covering on the star lattice. Dimers are shown as thick lines. Bottom: The same dimer covering in the arrow representation.

In the arrow representation for the star lattice, an arrow is located on each lattice site. It can point in one of two directions: either towards the center of the triangle to which the site belongs, or in the opposite direction, towards the center of the site's linking bond. In the first case the dimer that touches the site lies on one of the site's two triangle bonds. In the second case the dimer lies on the site's linking bond. If a triangle contains a dimer on bond  $ij$  the arrows on sites  $i$  and  $j$  both point into the triangle while the arrow on the triangle's third site points out of the triangle. In contrast, if a triangle has no dimer, all three arrows point out of the triangle. As these are the only possibilities, each triangle must satisfy the constraint that an even number (0 or 2) of its arrows must point into the triangle. Next consider a linking bond  $kl$ . If it has a dimer, the arrows on sites  $k$  and  $l$  both point "into" (i.e. towards the center of) the linking bond. Alternatively, the linking bond has no dimer, in which case the directions of both arrows are reversed to point "out of" (i.e. away from the center of) the linking bond. Hence each linking bond must satisfy the constraint that an even number (0 or 2) of its arrows must point "into" the bond. The constraint on a triangle is exactly the same as for the lattices of corner-sharing triangles for which the arrow representation has

been used earlier. Furthermore, the new constraint introduced for linking bonds takes the same form as the triangle constraint: an even number of arrows must point inwards. An example of a dimer covering and its arrow representation is given in Fig. 2.

### III. PSEUDO-SPIN REPRESENTATION OF DIMER COVERINGS AND AN EXACTLY SOLVABLE QUANTUM DIMER MODEL

Elser and Zeng introduced an Ising pseudo-spin representation for dimer coverings on the kagome lattice.<sup>21</sup> Misguich *et al.*<sup>19,22</sup> developed this representation further by unveiling additional important properties. In this section we show that an analogous pseudo-spin representation exists for the star lattice.<sup>38</sup> In Secs. III A and III B we derive the properties of this representation. In Sec. III C we use the pseudo-spin representation to define a star lattice QDM whose eigenstates and energy spectrum are exactly known and which has a Rokhsar-Kivelson ground state. This model has previously been discussed by Moessner and Sondhi from a different point of view.<sup>11</sup>

#### A. The operators $\hat{\sigma}^z(D)$

We consider a star lattice on a closed surface, i.e. a system without boundaries. The dimer coverings (DCs) can be grouped into topological sectors. To do this one looks at the transition graph of two DCs obtained by superposing them on top of each other. These transition graphs may contain two different types of non-intersecting even-length closed loops: loops that enclose a nonzero area and loops that enclose zero area (loops of the latter type have length 2). Loops of the first type can be topologically trivial or nontrivial (all loops of the second type are obviously topologically trivial).<sup>39</sup> If the transition graph of two DCs has no topologically non-trivial loops, these DCs are in the same topological sector.

Next consider a given topological sector for DCs on the star lattice. Let  $|c_0\rangle$  be some arbitrary but specific DC in this topological sector; it will play the role of a reference DC. Introduce a spin-1/2 operator  $\hat{\sigma}^z(D)$  for each dodecagon  $D$  with eigenvalues  $\sigma^z(D) = \pm 1$ . To any DC  $|c\rangle$  in the same topological sector as  $|c_0\rangle$  we can associate a pair of pseudo-spin configurations (PSCs)  $\{\sigma^z(D)\}$  and  $\{-\sigma^z(D)\}$  related by a global spin reversal, as follows: Draw the transition graph  $\langle c_0|c\rangle$ . Consider the closed loops that enclose a nonzero area in this graph; these loops are taken to be domain walls separating dodecagons with opposite values of  $\sigma^z$ .<sup>40</sup> The need to identify the two PSCs related by a global spin reversal with the same DC is due to the fact that the domain walls only determine the value of the products  $\sigma^z(D)\sigma^z(D')$  for all dodecagons  $D, D'$ , which are invariant under a global spin reversal. The reference DC  $|c_0\rangle$  is associated with the pair of PSCs

having all  $\sigma^z$  up and all  $\sigma^z$  down.

The mapping from DCs in a given topological sector to pairs of PSCs can also be formulated in terms of the arrow representation. Let  $D$  and  $D'$  be two neighboring dodecagons and consider the linking bond separating  $D$  and  $D'$ . If the two arrows associated with this linking bond point in opposite (the same) directions in  $|c\rangle$  and  $|c_0\rangle$ , there will (will not) be a domain wall between  $D$  and  $D'$  in the transition graph  $\langle c_0|c\rangle$ , so that the product  $\sigma^z(D)\sigma^z(D') = -1$  ( $1$ ) in the pair of PSCs associated with  $|c\rangle$ .

Two different DCs  $|c\rangle$  and  $|c'\rangle$  in the same topological sector will map to different pairs of PSCs. To see this we note that if the DCs are different, there will be some linking bonds that are occupied by a dimer in  $|c\rangle$  but unoccupied in  $|c'\rangle$  and vice versa. (In other words, it is impossible to have dimer coverings that differ only in the dimer occupation numbers on triangle bonds). Thus the arrows on these linking bonds point in opposite directions in  $|c\rangle$  and  $|c'\rangle$ , and therefore the product  $\sigma^z(D)\sigma^z(D')$  for the dodecagons  $D$  and  $D'$  separated by each such linking bond will be different for the PSCs of  $|c\rangle$  and  $|c'\rangle$ .

Any pair of PSCs related by global spin reversal corresponds to a unique DC  $|c\rangle$  in the topological sector of  $|c_0\rangle$  (this DC will however depend on the choice of  $|c_0\rangle$ ). To see this we note that given these PSCs we can find the value of the product  $\sigma^z(D)\sigma^z(D')$  for each neighboring pair of dodecagons  $D$  and  $D'$ . If the product is  $-1$  ( $1$ ) the directions of the two arrows on the linking bond separating  $D$  and  $D'$  are opposite (the same) in  $|c\rangle$  and  $|c_0\rangle$ . Since every arrow is associated with a unique linking bond in this way, all arrows are assigned a direction by this procedure, thus uniquely specifying  $|c\rangle$ .

From this mapping between DCs in a given topological sector and pairs of PSCs  $\{\sigma^z(D)\}$  and  $\{-\sigma^z(D)\}$ , it follows that the number of DCs in a topological sector of the star lattice is the same for each sector and given by  $2^{N_D-1}$  where  $N_D$  is the number of dodecagons. This result can be expressed in terms of the number of sites  $N$  and the genus  $g$  of the manifold by using Euler's formula  $V + F - E = \chi$  where  $V, F$ , and  $E$  are the number of vertices, faces, and edges in the lattice graph and the Euler characteristic  $\chi = 2 - 2g$  for a closed orientable surface of genus  $g$ . Here  $V = N$ ,  $F = N_D + N_T$  where  $N_T = N/3$  is the number of triangles, and  $E = N_t + N_l$  where  $N_t = 3N_T = N$  is the number of triangle bonds and  $N_l = N/2$  is the number of linking bonds. This gives  $N_D = N/6 + 2 - 2g$  so the number of DCs in each topological sector is  $2^{N/6+1-2g}$ . In Sec. IV A we will show that the total number of DCs on this lattice graph (i.e. including all topological sectors) is  $2^{N/6+1}$ . Thus the number of topological sectors is  $2^{N/6+1}/2^{N/6+1-2g} = 2^{2g} = 4^g$ , which is the expected result for a non-bipartite lattice on a genus- $g$  manifold.

## B. The operators $\hat{\sigma}^x(D)$

Using the arrow constraints, one finds that there are 64 different configurations for the 18 arrows on the six triangles that surround a given dodecagon. Each of these arrow configurations corresponds, in the dimer picture, to a “flippable”<sup>20</sup> dimer configuration along one of the 32 even-length loops that enclose the dodecagon and an even number of its six surrounding triangles (for each such loop there are two flippable dimer configurations). There is 1 loop of length 12, 15 loops of length 14, 15 loops of length 16, and 1 loop of length 18. The loops in these four classes surround the dodecagon and 0, 2, 4, and 6 of its neighboring triangles, respectively.

We now define the operator  $\hat{\sigma}^x(D)$  as

$$\hat{\sigma}^x(D) = \sum_{\alpha} (|L_{\alpha}(D)\rangle\langle\bar{L}_{\alpha}(D)| + \text{h.c.}). \quad (1)$$

This definition is analogous to the one for the kagome lattice.<sup>19,22</sup> The sum runs over the 32 even-length loops associated with  $D$ .  $|L_{\alpha}(D)\rangle$  and  $|\bar{L}_{\alpha}(D)\rangle$  are the two “flippable” dimer configurations along loop  $\alpha$  around dodecagon  $D$ . It can be seen that, in the arrow representation,  $\hat{\sigma}^x(D)$  flips the direction of the 12 arrows sitting on the dodecagon  $D$ . This operation respects the arrow constraints since it flips an even number (0 or 2) of the arrows involved in each arrow constraint in the system. From this result it immediately follows that  $(\hat{\sigma}^x(D))^2 = I$  (flipping the arrows twice is equivalent to doing nothing) and that  $[\hat{\sigma}^x(D), \hat{\sigma}^x(D')] = 0$  (it doesn’t matter in which order the arrows are flipped).

Next let  $D'$  be any of the dodecagons neighboring  $D$ . Consider the effect of acting with  $\hat{\sigma}^x(D)$  on a DC  $|c\rangle$  in the same topological sector as  $|c_0\rangle$ . If the directions of the two arrows on the linking bond separating  $D$  and  $D'$  are opposite (the same) in  $|c\rangle$  and  $|c_0\rangle$ , they will be the same (opposite) in  $\hat{\sigma}^x(D)|c\rangle$  and  $|c_0\rangle$ . Thus for all  $D'$  that neighbor  $D$ ,  $\hat{\sigma}^x(D)$  anticommutes with  $\hat{\sigma}^z(D)\hat{\sigma}^z(D')$ . Furthermore, if  $D_a$  and  $D_b$  are two neighboring dodecagons, both different from  $D$ , then  $\hat{\sigma}^z(D_a)\hat{\sigma}^z(D_b)$  clearly commutes with  $\hat{\sigma}^x(D)$  since the latter doesn’t affect the arrows on the linking bond separating  $D_a$  and  $D_b$ . These two results can be generalized<sup>41</sup> to, respectively,  $D'$  not a neighbor of  $D$  and  $D_a$  and  $D_b$  not neighbors of each other. From this we conclude that  $\hat{\sigma}^x(D)$  anticommutes with  $\hat{\sigma}^z(D)$  and commutes with  $\hat{\sigma}^z(D')$  for  $D' \neq D$ . This shows that (as implied by the notation)  $\hat{\sigma}^x(D)$  is the spin-1/2 operator that flips the pseudo-spin  $\sigma^z(D)$  at dodecagon  $D$ . Also note that

$$\prod_D \hat{\sigma}^x(D) = I. \quad (2)$$

This constraint involving all dodecagons follows from the fact that  $\prod_D \hat{\sigma}^x(D)$  is the operator that effects a global spin reversal, under which a PSC  $\{\sigma^z(D)\}$  maps to its partner  $\{-\sigma^z(D)\}$  that represents the same DC. Alternatively, this constraint can be understood from the arrow

representation, since the lhs of Eq. (2) flips all arrows twice and therefore is equivalent to doing nothing.

Starting from the arrow representation for the reference DC  $|c_0\rangle$ , and given one of the two PSCs for the DC  $|c\rangle$  in the same sector, the arrow representation for  $|c\rangle$  can be obtained either by applying  $\hat{\sigma}^x$  to  $|c_0\rangle$  at all dodecagons with  $\sigma^z = +1$  in  $|c\rangle$  or by applying  $\hat{\sigma}^x$  to  $|c_0\rangle$  at all dodecagons with  $\sigma^z = -1$  in  $|c\rangle$ . Either way, the arrows that point in different directions in  $|c_0\rangle$  and  $|c\rangle$  will be flipped once, while the arrows that point in the same direction in  $|c_0\rangle$  and  $|c\rangle$  will be flipped zero or two times.

## C. An exactly solvable quantum dimer model

Given the form of  $\hat{\sigma}^x(D)$ , it is natural to consider a QDM defined by the Hamiltonian

$$\hat{H} = -\Gamma \sum_D \hat{\sigma}^x(D) \quad (3)$$

with  $\Gamma$  a positive constant. This QDM, which has no potential energy terms, is the star-lattice analogue of the kagome lattice QDM introduced by Misguich *et al.*<sup>19</sup> It has been discussed previously by Moessner and Sondhi<sup>11</sup> as a particular limit of a QDM they arrived at via a mapping (based on a modified Fisher construction) to a three-dimensional Ising model in the time-continuum limit.

Let us discuss some basic properties of the QDM (3) from the point of view of the pseudo-spin representation that we have introduced in this section. Clearly the eigenstates are of the form  $\prod_D |\sigma^x(D)\rangle$  where  $|\sigma^x(D)\rangle$  is an eigenstate of  $\hat{\sigma}^x(D)$  with eigenvalue  $\sigma^x(D) = \pm 1$ . Note however that due to the constraint (2), only eigenstates with an *even* number of dodecagons in the excited  $\sigma^x = -1$  state are allowed. These  $\sigma^x = -1$  excitations localized at the dodecagons are (point) visons.<sup>11,19</sup> We will discuss them further in Sec. VIII. In the ground state, each dodecagon is in the  $\sigma^x = +1$  state which is just the sum of the  $\sigma^z = +1$  and  $\sigma^z = -1$  eigenstates. Expanding out the product over dodecagons, the ground state is seen to be the equal-amplitude superposition of all dimer coverings in a given topological sector, i.e. the RK state. Since the ground state energy is the same in each of the  $4^g$  topological sectors the system has topological order.<sup>16,42</sup> (Note that the ground state is degenerate even for a system with a finite number of sites.)

The fact that the ground state is  $4^g$ -fold degenerate can also be seen as follows: A ground state  $|\Psi_0\rangle$  of (3) satisfies  $\hat{\sigma}^x(D)|\Psi_0\rangle = |\Psi_0\rangle$  for each dodecagon  $D$ . This can be regarded as a constraint on  $|\Psi_0\rangle$ . There is one such constraint for each dodecagon. However, due to (2) only  $N_D - 1$  of these constraints are independent. Every independent dodecagon constraint reduces the number of possible states in the ground state manifold by a factor of two, since it specifies one of two possible eigenstates at that dodecagon. As in Sec. III A we invoke the result

to be shown in Sec. IV A, that the total number of dimer coverings is  $2^{N/6+1}$  which is therefore also the dimension of the Hilbert space. Thus the dimension of the ground state manifold is  $2^{N/6+1-(N_d-1)} = 4^g$ , where we used  $N_D = N/6 + 2 - 2g$  as shown in Sec. III A.

As noted in the introduction, RK-state correlations involving operators that are diagonal in the dimer basis are given by the corresponding correlation functions in the CDM with equal dimer weights. This CDM will be analyzed in the following sections.

#### IV. THE NUMBER OF DIMER COVERINGS

In this section we consider the number of dimer coverings  $\mathcal{Z}$  on a star lattice graph with a finite number of sites  $N$ . We will take the graph to be embedded on a closed surface so that the system has no boundaries. We first consider a surface of arbitrary genus  $g$  and give a derivation of  $\mathcal{Z}$  based on the arrow representation introduced in Sec. II. Next we calculate  $\mathcal{Z}$  for a torus (genus  $g = 1$ ) using the Pfaffian method. Some alternative derivations of this result are discussed in Sec. XI and Appendix A.

##### A. Arrow derivation for a genus- $g$ manifold

Consider a star lattice graph embedded on a closed orientable surface of genus  $g$ . If this graph has  $N$  sites there are  $N/3$  triangles and  $N/2$  linking bonds. As the two latter numbers must both be integers,  $N$  is a multiple of 6 (and thus also even). Since there is one arrow per site and each arrow is an Ising variable (i.e. it can point in two different directions) it follows that in the absence of any constraints there would be  $2^N$  different ways to choose the directions of the arrows. Each of the triangles and linking bonds does however contribute an arrow constraint, giving a total of  $N/3 + N/2 = 5N/6$  constraints. As will be shown below, one of these constraints can be deduced from the others, leaving  $5N/6 - 1$  independent constraints, each of which can be used to eliminate exactly one arrow variable.<sup>44</sup> Thus the total number of dimer coverings on this star lattice graph is

$$\mathcal{Z} = 2^{N-(5N/6-1)} = 2^{N/6+1}. \quad (4)$$

We note that the result is independent of the genus  $g$ . The associated entropy  $\mathcal{S} = \log \mathcal{Z}$  is thus

$$\mathcal{S} = \frac{\log 2}{6} N + \log 2. \quad (5)$$

As shown in Sec. III A there are  $4^g$  topological sectors, each of which have the same number of dimer coverings  $\mathcal{Z}_{\text{ts}} = \mathcal{Z}/4^g$ . The corresponding entropy per sector is therefore

$$\mathcal{S}_{\text{ts}} = \frac{\log 2}{6} N + (1 - 2g) \log 2. \quad (6)$$

From these expressions one sees that the entropy per site in the thermodynamic limit is given by  $(1/6) \log 2$ , in agreement with previous calculations.<sup>3,45</sup> In addition to the leading  $O(N)$  (i.e., extensive) term the entropy also has a sub-leading  $O(1)$  term that carries information about the topology of the system.

Let us show that only  $5N/6 - 1$  arrow constraints are independent as claimed above. Consider an arbitrary site  $i$ . Denote the triangle and the linking bond it belongs to by  $T$  and  $l$  respectively. Define the arrow variable  $a_{i,T} = +1$  ( $-1$ ) if the arrow on site  $i$  points out of (into)  $T$ . Similarly, define the arrow variable  $a_{i,l} = +1$  ( $-1$ ) if the arrow points out of (into)  $l$ . Clearly these two variables are related by  $a_{i,T} = -a_{i,l}$ . Furthermore define  $a_T = \prod_{i \in T} a_{i,T}$  where the product runs over the three sites belonging to the triangle  $T$ , and  $a_l \equiv \prod_{i \in l} a_{i,l}$  where the product runs over the two sites belonging to the linking bond  $l$ . We have

$$\left( \prod_T a_T \right) \left( \prod_l a_l \right) = \prod_{i=1}^N a_{i,T} a_{i,l} = (-1)^N = 1. \quad (7)$$

On the other hand, the  $5N/6$  arrow constraints can be written

$$a_T = a_l = 1 \text{ for all } T, l. \quad (8)$$

From (7) we see that one of the constraints in (8) follows from the others, leaving  $5N/6 - 1$  independent constraints.

##### B. Pfaffian calculation for a torus

The Pfaffian method can be used to calculate the number of dimer coverings  $\mathcal{Z}$  on any planar lattice graph.<sup>9</sup> In this method the central object is an antisymmetric matrix  $A$ , sometimes called a Kasteleyn matrix, whose dimension equals the (even) number of sites  $N$ . The matrix element  $A_{ij}$  is nonzero only if sites  $i$  and  $j$  are connected by a bond in the lattice graph, in which case the magnitude of  $A_{ij}$  is set equal to 1.<sup>46</sup> The sign of  $A_{ij}$  defines the direction of an arrow<sup>47</sup> on the bond  $ij$ : If  $A_{ij} > 0$  the arrow points from  $i$  to  $j$ . The signs of the matrix elements of  $A$  should be chosen to satisfy Kasteleyn's clockwise-odd rule:<sup>9,48</sup> The perimeter of each face of the lattice graph should contain an odd number of arrows pointing in the clockwise direction around the face. One then has  $\mathcal{Z} = |\text{Pf } A|$ , where  $\text{Pf } A$  is the Pfaffian of  $A$ . Using  $(\text{Pf } A)^2 = \det A$  it follows that  $\mathcal{Z} = \sqrt{\det A}$  for a planar lattice graph.

Fisher<sup>10</sup> and Wu<sup>3</sup> have used the Pfaffian method to calculate the free energy per site/dimer for the dimer problem on an *infinite* star lattice. For our Pfaffian calculations we follow Fisher in viewing the star lattice as a square lattice of 6-site unit cells, as shown in Fig. 3, where we also use his labeling of sites and choice of bond arrow directions to satisfy Kasteleyn's sign rule. A site

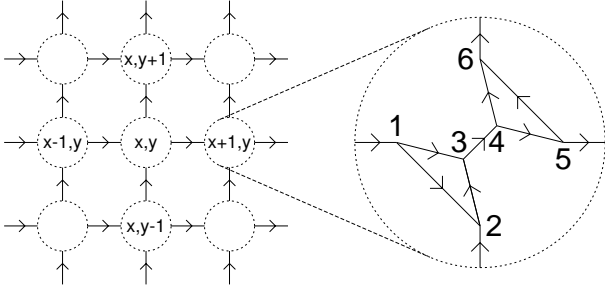


FIG. 3: The star lattice drawn as a square lattice (left) of 6-site unit cells (right). Also shown are the directions of the Kasteleyn arrows and the labeling of unit cells and sites within a unit cell. These conventions follow Ref. 10.

$i$  is written  $i = \mathbf{r}, \alpha$  where  $\alpha = 1, \dots, 6$  is the site label within the unit cell, and  $\mathbf{r} = (x, y)$  labels the unit cell, where  $x = 1, \dots, N_x$  is the horizontal coordinate and  $y = 1, \dots, N_y$  the vertical one, with  $N_x$  and  $N_y$  being the number of unit cells in the horizontal and vertical direction, respectively. The total number of sites in the lattice is then  $N = 6N_xN_y$ , which is always even so that the lattice can be completely covered by dimers for any choice of  $N_x$  and  $N_y$ .

When the sites on opposite edges in the two directions are connected by additional bonds to form a torus, the resulting lattice graph is no longer planar. However, as shown by Kasteleyn,<sup>6</sup> the dimer problem on a torus can still be solved using Pfaffians by a small modification of the procedure described so far. In this case  $\mathcal{Z}$  can be expressed as a linear combination of the Pfaffians of four different Kasteleyn matrices  $A^{\nu_x\nu_y}$  ( $\nu_x, \nu_y = 0, 1$ ), where the first (second) superscript on  $A^{\nu_x\nu_y}$  labels the type of boundary condition imposed on the matrix elements in the horizontal (vertical) direction. Compared to the single Kasteleyn matrix for the open-boundary case, these four matrices differ only in the presence of additional nonzero matrix elements corresponding to the additional bonds introduced to establish the torus geometry. Specifically, the new matrix elements of  $A^{\nu_x\nu_y}$  are given by

$$A_{N_x, y, 5; 1, y, 1}^{\nu_x\nu_y} = (-1)^{\nu_x} \quad \text{for all } y, \quad (9)$$

$$A_{x, N_y, 6; x, 1, 2}^{\nu_x\nu_y} = (-1)^{\nu_y} \quad \text{for all } x, \quad (10)$$

with  $A_{ij}^{\nu_x\nu_y} = -A_{ji}^{\nu_x\nu_y}$ . From the arrows in Fig. 3 one sees that the value 0 (1) for  $\nu_x, \nu_y$  implies periodic (anti-periodic) boundary conditions on the matrix elements. On the torus one then has<sup>6</sup> (see also Ref. 49)

$$\mathcal{Z} = \frac{1}{2} \sum_{\nu_x, \nu_y=0,1} r_{\nu_x\nu_y} \sqrt{\det A^{\nu_x\nu_y}}, \quad (11)$$

where  $r_{\nu_x\nu_y}$  are signs whose values will be determined below.

In order to calculate these determinants, as well as other quantities to be considered later, we will use

Samuel's reformulation of the Pfaffian method in terms of a path integral description of noninteracting Majorana fermions living on the lattice sites.<sup>33</sup> A fermion on site  $i$  is associated with a Grassmann variable  $\psi_i$ . The action  $S$  of the fermions is defined in terms of a Kasteleyn matrix  $A$  of the dimer problem,

$$S = \frac{1}{2} \sum_{ij} \psi_i A_{ij} \psi_j. \quad (12)$$

The partition function  $Z$  of the fermions then equals the Pfaffian of  $A$ ,

$$Z = \int \mathcal{D}\psi \exp(-S) = \text{Pf } A. \quad (13)$$

Here  $\int \mathcal{D}\psi \equiv \int d\psi_1 \dots d\psi_N$ . In the following the matrix  $A$  is taken to be one of the four Kasteleyn matrices  $A^{\nu_x\nu_y}$  for the dimer problem on the torus. To avoid cluttering the notation we will however not write the superscripts explicitly. We first introduce new Grassmann variables  $\tilde{\psi}_{\mathbf{k}, \alpha}$  related to the  $\psi_{\mathbf{r}, \alpha}$  by a Fourier transformation,

$$\psi_{\mathbf{r}, \alpha} = \frac{1}{\sqrt{N_x N_y}} \sum_{\mathbf{k}} e^{i\mathbf{k} \cdot \mathbf{r}} \tilde{\psi}_{\mathbf{k}, \alpha}. \quad (14)$$

The form of the wavevectors  $\mathbf{k}$  depends on the boundary conditions  $\nu_x$  and  $\nu_y$ , i.e.  $k_x = 2\pi(n_x + \nu_x/2)/N_x$  and similarly for  $k_y$ . The integers  $n_x$  and  $n_y$  are chosen so that the sum over  $\mathbf{k}$  runs over the first Brillouin zone. The partition function can now be written  $Z = \int \mathcal{D}\tilde{\psi} \exp(-S)$  with

$$S = \frac{1}{2} \sum_{\mathbf{k}} \sum_{\alpha\beta} \tilde{\psi}_{-\mathbf{k}, \alpha} \tilde{A}(\mathbf{k})_{\alpha\beta} \tilde{\psi}_{\mathbf{k}, \beta}, \quad (15)$$

where  $\tilde{A}(\mathbf{k})$  is the  $6 \times 6$  matrix

$$\tilde{A}(\mathbf{k}) = \begin{pmatrix} 0 & 1 & 1 & 0 & -e^{-ik_x} & 0 \\ -1 & 0 & 1 & 0 & 0 & -e^{-ik_y} \\ -1 & -1 & 0 & 1 & 0 & 0 \\ 0 & 0 & -1 & 0 & 1 & 1 \\ e^{ik_x} & 0 & 0 & -1 & 0 & 1 \\ 0 & e^{ik_y} & 0 & -1 & -1 & 0 \end{pmatrix}. \quad (16)$$

From (15) it then follows that  $\det A = Z^2$  is given by

$$\det A = \prod_{\mathbf{k}} \det \tilde{A}(\mathbf{k}). \quad (17)$$

Because  $\det \tilde{A}(\mathbf{k}) = 4$  for all  $\mathbf{k}$ ,  $\det A = 4^{N_x N_y} = 4^{N/6}$  independently of the boundary conditions  $\nu_x$  and  $\nu_y$ . Thus (11) becomes  $\mathcal{Z} = (r/2) \cdot 2^{N/6}$  where  $r \equiv r_{00} + r_{01} + r_{10} + r_{11}$ . We expect  $r$  to contribute to an  $N$ -independent term in the entropy (cf. Eqs. (5)-(6)). Thus  $r$  can be determined by manually counting the number of dimer coverings for a torus with only one unit cell<sup>49</sup> (i.e.  $N = 6$ ). We find  $\mathcal{Z} = 4$  for this case, which implies  $r = 4$ , i.e. all

terms in (11) come with a positive sign. Thus the number of dimer coverings on a star lattice on a torus with  $N$  sites is given by<sup>38</sup>

$$\mathcal{Z} = 2^{N/6+1}, \quad (18)$$

in agreement with the result (4) derived from the arrow representation in Sec. IV A.

## V. THE GREEN FUNCTION

Within the framework of the fermionic formulation of the Pfaffian method,<sup>33</sup> quantities of interest for the dimer problem can be expressed in terms of fermionic correlation functions.<sup>2,24,33,50</sup> The average number of dimers on a bond is given directly as the two-point Green function of the Majorana fermions. Furthermore, dimer, vison, and monomer correlation functions can be expressed in terms of multi-point Green functions, which in turn, by Wick's theorem, are given as sums of products of two-point Green functions. In this section we calculate the two-point Green function of the star-lattice CDM for the case of equal dimer weights.

The expectation value of an arbitrary operator  $O$  in the fermionic system defined by (12) and (13) is  $\langle O \rangle =$

$Z^{-1} \int \mathcal{D}\psi O \exp(-S)$ . The two-point Green function (henceforth just called the Green function) is then

$$G_{ij} \equiv \langle \psi_i \psi_j \rangle = (A^{-1})_{ij}. \quad (19)$$

Thus, viewed as a matrix, the Green function is the inverse of the Kasteleyn matrix:  $G = A^{-1}$ . Using Eq. (14), one can write  $G_{\mathbf{r},\alpha;\mathbf{r}',\alpha'} = \langle \psi_{\mathbf{r},\alpha} \psi_{\mathbf{r}',\alpha'} \rangle = (N_x N_y)^{-1} \sum_{\mathbf{k},\mathbf{k}'} e^{i(\mathbf{k}\cdot\mathbf{r}+\mathbf{k}'\cdot\mathbf{r}')} \langle \tilde{\psi}_{\mathbf{k},\alpha} \tilde{\psi}_{\mathbf{k}',\alpha'} \rangle$ . From Eq. (15) one finds  $\langle \tilde{\psi}_{\mathbf{k},\alpha} \tilde{\psi}_{\mathbf{k}',\alpha'} \rangle = \delta_{\mathbf{k}',-\mathbf{k}} \tilde{A}^{-1}(\mathbf{k})_{\alpha\alpha'}$ , where  $\tilde{A}^{-1}(\mathbf{k})$  is the inverse matrix of  $\tilde{A}(\mathbf{k})$ . Thus

$$G_{\mathbf{r},\alpha;\mathbf{r}',\alpha'} = \int_{-\pi}^{\pi} \frac{dk_x}{2\pi} \int_{-\pi}^{\pi} \frac{dk_y}{2\pi} e^{i\mathbf{k}\cdot(\mathbf{r}-\mathbf{r}')} \tilde{A}^{-1}(\mathbf{k})_{\alpha\alpha'} \quad (20)$$

where we have also taken the thermodynamic limit  $N_x, N_y \rightarrow \infty$ . In this limit the Green function becomes independent of the boundary conditions  $\nu_x, \nu_y$  because the wavevectors are no longer discrete. The inverse matrix of  $\tilde{A}(\mathbf{k})$  takes the form

$$\tilde{A}^{-1}(\mathbf{k}) = \frac{1}{4} \begin{pmatrix} P & -R^\dagger \\ R & Q \end{pmatrix} \quad (21)$$

where  $P, Q$ , and  $R$  are  $3 \times 3$  matrices given by

$$P = \begin{pmatrix} e^{ik_y} - e^{-ik_y} & -1 - e^{-ik_x} - e^{ik_y} + e^{-ik_x+ik_y} & -1 + e^{-ik_x} - e^{-ik_y} - e^{-ik_x+ik_y} \\ 1 + e^{ik_x} + e^{-ik_y} - e^{ik_x-ik_y} & -e^{ik_x} + e^{-ik_x} & -1 - e^{-ik_x} + e^{-ik_y} - e^{ik_x-ik_y} \\ 1 - e^{ik_x} + e^{ik_y} + e^{ik_x-ik_y} & 1 + e^{ik_x} - e^{ik_y} + e^{-ik_x+ik_y} & e^{ik_x-ik_y} - e^{-ik_x+ik_y} \end{pmatrix}, \quad (22)$$

$$Q = \begin{pmatrix} -e^{ik_x-ik_y} + e^{-ik_x+ik_y} & -1 + e^{-ik_x} - e^{-ik_y} - e^{-ik_x+ik_y} & -1 - e^{-ik_x} + e^{-ik_y} - e^{ik_x-ik_y} \\ 1 - e^{ik_x} + e^{ik_y} + e^{ik_x-ik_y} & -e^{ik_y} + e^{-ik_y} & -1 - e^{ik_x} - e^{-ik_y} + e^{ik_x-ik_y} \\ 1 + e^{ik_x} - e^{ik_y} + e^{-ik_x+ik_y} & 1 + e^{-ik_x} + e^{ik_y} - e^{-ik_x+ik_y} & e^{ik_x} - e^{-ik_x} \end{pmatrix}, \quad (23)$$

$$R = \begin{pmatrix} 1 + e^{ik_x} + e^{ik_y} - e^{ik_x-ik_y} & -1 - e^{ik_x} - e^{ik_y} + e^{-ik_x+ik_y} & 2 - e^{ik_x-ik_y} - e^{-ik_x+ik_y} \\ -2e^{ik_x} + e^{ik_x+ik_y} + e^{ik_x-ik_y} & 1 + e^{ik_x} + e^{ik_y} - e^{ik_x+ik_y} & -1 - e^{ik_x} - e^{ik_y} + e^{ik_x-ik_y} \\ 1 + e^{ik_x} + e^{ik_y} - e^{ik_x+ik_y} & -2e^{ik_y} + e^{ik_x+ik_y} + e^{-ik_x+ik_y} & 1 + e^{ik_x} + e^{ik_y} - e^{-ik_x+ik_y} \end{pmatrix}. \quad (24)$$

Since the dependence on  $\mathbf{r}, \mathbf{r}'$  in Eq. (20) is only through  $\mathbf{r} - \mathbf{r}' \equiv \mathbf{R}$ , we define  $G_{\mathbf{r},\alpha;\mathbf{r}',\alpha'} \equiv G(\mathbf{R})_{\alpha\alpha'} = G(R_x, R_y)_{\alpha\alpha'}$ . We see from Eqs. (21)-(24) that each term in the matrix elements of  $\tilde{A}^{-1}(\mathbf{k})$  contains at most one power of  $e^{\pm ik_x}$  and at most one power of  $e^{\pm ik_y}$ . From Eq. (20) it then follows that

$$G(R_x, R_y)_{\alpha\alpha'} = 0 \quad \text{if } |R_x| \geq 2 \text{ or if } |R_y| \geq 2, \quad (25)$$

i.e. the Green function vanishes identically beyond a very short distance. The same property has recently also been found for the Green function on the kagome lattice.<sup>23,24</sup>

For each  $\mathbf{R}$ ,  $G(\mathbf{R}) = G(R_x, R_y)$  defines a  $6 \times 6$  matrix. Of these, due to Eq. (25), only  $G(0,0)$ ,  $G(1,0)$ ,  $G(-1,0)$ ,  $G(0,1)$ ,  $G(0,-1)$ ,  $G(-1,1)$ ,  $G(1,-1)$ ,  $G(1,1)$  and  $G(-1,-1)$  can be nonzero. However, not all of these

matrices are independent because  $G = A^{-1}$  is antisymmetric and thus  $G(-R_x, -R_y) = -G(R_x, R_y)^T$ .

The results for the Green function obtained in this section will be used in the fermionic calculations of the quantities considered in Secs. VI-IX.

## VI. DIMER OCCUPATION PROBABILITIES

Let  $i$  and  $j$  be two sites connected by a bond. Since for any dimer covering of the lattice, the bond  $ij$  is either occupied by a dimer or not, the number of dimers  $n_{ij}$  on the bond can only take the values 0 or 1. We define  $p(ij) = \langle n_{ij} \rangle$  as the average of  $n_{ij}$  over all dimer coverings. Thus  $p(ij)$  is the probability that bond  $ij$  is



occupied by a dimer. For the star lattice with the same dimer weight on all bonds, symmetry dictates that  $p(ij)$  may take at most two different values as the bond  $ij$  is varied:  $p(ij) = p_t$  if  $ij$  is a triangle bond and  $p(ij) = p_l$  if  $ij$  is a linking bond. Explicit calculations give

$$p_t = \frac{1}{4}, \quad p_l = \frac{1}{2} \quad (26)$$

Before turning to the derivation of this result, let us show that  $p_t$  and  $p_l$  are related to each other. This can be seen by considering the average number of dimers in the whole system, given by  $\langle \sum_{(ij)} n_{ij} \rangle = Np_t + (N/2)p_l$ . Here the sum goes over all bonds and the prefactors of  $p_t$  and  $p_l$  are the number of triangle bonds and linking bonds, respectively, in a system with  $N$  sites. The average is trivially equal to  $N/2$  since each dimer covering satisfies the close-packed hard-core constraint. Thus

$$p_t + \frac{1}{2}p_l = \frac{1}{2}. \quad (27)$$

### A. Fermionic approach

The probability  $p(ij)$  for having a dimer on bond  $ij$  is given by<sup>51</sup>

$$p(ij) = \langle n_{ij} \rangle = -\langle \psi_i \psi_j \rangle = -G_{ij}. \quad (28)$$

In this expression the site labels  $i$  and  $j$  have been chosen such that  $A_{ij} > 0$ , i.e. the Kasteleyn arrow goes from  $i$  to  $j$ . Eq. (28) can be derived<sup>24</sup> from the form of the generating function for dimer coverings when the dimer weights are allowed to be arbitrary (the dimer generating function reduces to our  $\mathcal{Z}$  when all dimer weights are equal). The result (26) now easily follows by using Eqs. (20)-(24) to evaluate Eq. (28).

### B. Arrow approach

The probability  $p(ij) = \langle n_{ij} \rangle$  of having a dimer on bond  $ij$  is given by the ratio

$$p(ij) = \frac{\mathcal{Z}(\{n_{ij} = 1\})}{\mathcal{Z}} \quad (29)$$

where  $\mathcal{Z}(\{n_{ij} = 1\})$  is the number of dimer coverings in which bond  $ij$  is occupied by a dimer and  $\mathcal{Z}$  is the total number of dimer coverings. In the sections that follow we will discuss other quantities that can be written in this way as well, i.e. as the ratio of a numerator, call it  $\mathcal{Z}'$  in general, and the denominator which is  $\mathcal{Z}$  in all cases. In Sec. IV A the latter was expressed as  $\mathcal{Z} = 2^{\mathcal{N}_a - \mathcal{N}_c}$  where  $\mathcal{N}_a$  is the number of flippable arrows (which are Ising (i.e.  $Z_2$ ) degrees of freedom) and  $\mathcal{N}_c$  is the number of independent constraints on these arrows. For all quantities of interest, the numerator  $\mathcal{Z}'$  can be expressed in terms of arrows in a completely analogous way, the only difference

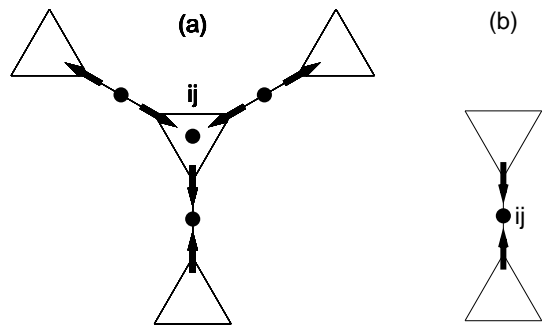


FIG. 4: The presence of a dimer on bond  $ij$  leads to a set of “spent” arrows and constraints as shown (the filled circles symbolize the constraints). This collection of arrows and constraints is referred to as the dimer’s imprint. (a) Imprint of a dimer on a triangle bond  $ij$ . (b) Imprint of a dimer on a linking bond  $ij$ . The probability  $p(ij)$  of having a dimer on the bond  $ij$  is found by inserting the number of spent arrows and constraints  $\Delta\mathcal{N}_a$  and  $\Delta\mathcal{N}_c$  into Eq. (30).

being that the calculation of  $\mathcal{Z}'$  corresponds to imposing additional requirements on some of these arrows. For example, some arrows may be required to point in definite directions. If these additional requirements are incompatible with the arrow constraints it follows that the numerator vanishes. If, on the other hand, they are compatible with the constraints, they will cause the number of remaining constraints and flippable arrows to change by  $\Delta\mathcal{N}_c$  and  $\Delta\mathcal{N}_a$ , respectively, compared to their values in the calculation of  $\mathcal{Z}$ . This gives the result

$$\frac{\mathcal{Z}'}{\mathcal{Z}} = 2^{\Delta\mathcal{N}_a - \Delta\mathcal{N}_c}. \quad (30)$$

The calculation of such a ratio therefore amounts to identifying the values of  $\Delta\mathcal{N}_a$  and  $\Delta\mathcal{N}_c$  for the quantity of interest.

Having explained the calculation in general, let us now apply this arrow approach to Eq. (29), for which the dimer coverings that contribute to the numerator are characterized by having a dimer on bond  $ij$ . Let us first consider the case of  $ij$  being a triangle bond. The presence of a dimer on such a bond implies that the arrows on site  $i$  and site  $j$  must both point into the associated triangle. The arrow constraint for the triangle then implies that the arrow on the third site of the triangle must point out of the triangle. Next, as each of the three fixed arrows on the triangle also belongs to a linking bond, the constraint on each of the three linking bonds fixes the direction of the arrow on the other end of the linking bond. Thus the directions of six arrows become fixed by having a dimer on the triangle bond  $ij$ . These arrows are therefore no longer flippable, Ising degrees of freedom, so  $\Delta\mathcal{N}_a = -6$ . Furthermore, four constraints are also spent (the triangle constraint and three linking bond constraints) so  $\Delta\mathcal{N}_c = -4$ . This gives  $p(ij) = 2^{-6 - (-4)} = 1/4 = p_t$ . This case is illustrated in

Fig. 4(a).

Next consider the case of  $ij$  being a linking bond. Having a dimer on such a bond implies that the two arrows must point into (towards the center of) the linking bond, giving  $\Delta\mathcal{N}_a = -2$ . Furthermore,  $\Delta\mathcal{N}_c = -1$  since the constraint on that linking bond is then spent. Thus  $p(ij) = 2^{-2-(-1)} = 1/2 = p_l$ . This case is illustrated in Fig. 4(b).

The set of spent arrows and constraints that results from having a dimer on a given bond will be referred to as the dimer's *imprint*. Fig. 4(a) and (b) shows the dimer imprint for a triangle-bond dimer and a linking-bond dimer, respectively. Thus from counting the number of arrows and constraints in the imprint of a dimer on the bond  $ij$ , one can use Eq. (30) to calculate the probability  $p(ij)$  of having a dimer on that bond.

## VII. DIMER CORRELATIONS

In this section we consider correlations between dimers in the star-lattice CDM with equal dimer weights. The main focus is on correlations between two dimers, but at the end we also briefly discuss correlations between three dimers.

The probability that bonds  $ij$  and  $kl$  both have a dimer is given by  $p(ij, kl) = \langle n_{ij}n_{kl} \rangle$ . The correlations between dimers on bonds  $ij$  and  $kl$  are quantified by the dimer-dimer correlation function<sup>8</sup>

$$\begin{aligned} c(ij, kl) &= p(ij, kl) - p(ij)p(kl) \\ &= \langle n_{ij}n_{kl} \rangle - \langle n_{ij} \rangle \langle n_{kl} \rangle. \end{aligned} \quad (31)$$

This quantity can have either sign and vanishes for uncorrelated dimers. Our results for  $c(ij, kl)$  are presented in Fig. 5 (all numbers are in units of  $1/16$ ). We find that a dimer is uncorrelated with all dimers located further away than on one of the closest triangles. In particular, dimers on linking bonds are uncorrelated with each other.

### A. Fermionic approach

In the fermionic approach  $\langle n_{ij}n_{kl} \rangle$  is given by a four-point correlation function,<sup>51</sup>

$$\langle n_{ij}n_{kl} \rangle = \langle \psi_i \psi_j \psi_k \psi_l \rangle. \quad (32)$$

This expression for  $\langle n_{ij}n_{kl} \rangle$  can be derived from the generating function of dimer coverings in the same way as Eq. (28).<sup>24</sup> (In this derivation the site labels were chosen so that the two Kasteleyn arrows go from  $i$  to  $j$  and from  $k$  to  $l$ , respectively; cf. the remark after Eq. (28)). Since the fermionic action is quadratic, the four-point function  $\langle \psi_i \psi_j \psi_k \psi_l \rangle$  can be evaluated using Wick's theorem. Inserting the Wick expansion into Eq. (31) and using Eq. (28), the term  $G_{ij}G_{kl}$  cancels, giving

$$c(ij, kl) = G_{il}G_{jk} - G_{ik}G_{jl}. \quad (33)$$

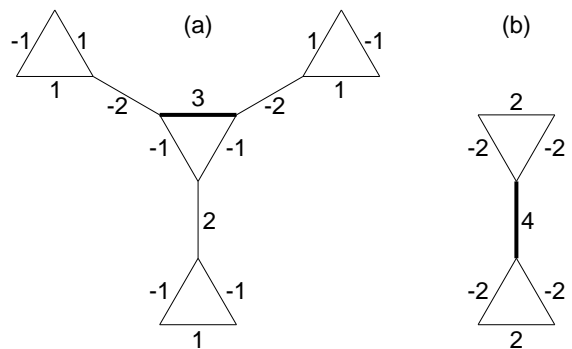


FIG. 5: Dimer-dimer correlations on the star lattice. The number next to a bond  $kl$  is the dimer-dimer correlation function  $c(ij, kl)$  (in units of  $1/16$ ) where the reference bond  $ij$  is shown in bold. (a) The reference bond is a triangle bond. (b) The reference bond is a linking bond. In both (a) and (b) only bonds  $kl$  with  $c(ij, kl) \neq 0$  are shown. Note that the correlations between dimers on different bond types can be read off from both (a) and (b).

The property (25) of the Green function then implies that also the dimer-dimer correlation function will vanish beyond a very short distance. (Note that Eq. (32) is not valid for the case  $ij = kl$  when one instead has  $\langle n_{ij}^2 \rangle = -G_{ij}$ , since  $n_{ij}^2 = n_{ij}$ . Thus  $c(ij, ij) = -G_{ij} - G_{ij}^2$ .) The results from the Green function calculation of the dimer-dimer correlation function are shown in Fig. 5.

### B. Arrow approach

The probability  $p(ij, kl) = \langle n_{ij}n_{kl} \rangle$  is given by

$$p(ij, kl) = \frac{\mathcal{Z}(\{n_{ij} = 1, n_{kl} = 1\})}{\mathcal{Z}} \quad (34)$$

where  $\mathcal{Z}(\{n_{ij} = 1, n_{kl} = 1\})$  is the number of dimer coverings with dimers on both  $ij$  and  $kl$ . Eq. (34) is a ratio of the type (30) that can be evaluated with the arrow representation as explained in Sec. VIB. One starts by laying down the imprints of spent arrows and constraints for each of the two dimers (these imprints are shown for the two types of dimers in Fig. 4). If the dimers are sufficiently far apart that their respective imprints have no arrows in common, the two dimers contribute additively to  $\Delta\mathcal{N}_a - \Delta\mathcal{N}_c$ . This gives  $p(ij, kl) = p(ij)p(kl)$ , i.e. the dimers are uncorrelated.<sup>52</sup> In contrast, dimers are correlated if their imprints overlap. In this situation  $p(ij, kl) = 0$  if the overlapping parts do not match, which happens if the two dimers cannot both be present in a dimer covering. Alternatively, if the overlapping parts do match, the value of  $\Delta\mathcal{N}_a - \Delta\mathcal{N}_c$  is larger (i.e., less negative) than the sum of the contributions from each dimer considered separately, thus giving  $p(ij, kl) > p(ij)p(kl)$ . This arrow calculation reproduces the results for  $c(ij, kl)$  shown in Fig. 5. Note that a dimer on a triangle bond

(Fig. 5(a)) is correlated with dimers further away than a dimer on a linking bond is (Fig. 5(b)). This difference is a consequence of the different sizes of their respective imprints shown in Fig. 4. In particular, the imprint of linking bond dimers is so small that such dimers are only correlated with dimers on the two triangles touching the linking bond. Dimers on triangle bonds, having a somewhat bigger imprint, are correlated only if they are on the same or neighboring triangles.

The notion of an imprint can be generalized to more than one dimer. For example, the imprint of two dimers at  $ij$  and  $kl$  is given by the collection of spent arrows and constraints resulting from those two dimers. If the arrows are mutually compatible, the probability  $p(ij, kl)$  can be found by inserting the number of spent arrows and constraints into Eq. (30). Another example will be given in the next subsection.

### C. Correlations between three dimers

Correlations between three (or more) dimers can be similarly analyzed. Let us briefly consider the three-dimer case. This will involve the probability  $p(ij, kl, mn) = \langle n_{ij} n_{kl} n_{mn} \rangle$  that the bonds  $ij$ ,  $kl$ , and  $mn$  are all occupied by a dimer. Note that even if all three dimers are pairwise uncorrelated, i.e.  $p(ij, kl) = p(ij)p(kl)$ ,  $p(ij, mn) = p(ij)p(mn)$ , and  $p(kl, mn) = p(kl)p(mn)$ , it isn't necessarily true that  $p(ij, kl, mn)$  equals  $p(ij)p(kl)p(mn)$ . As an example, consider the situation with the bonds  $ij$ ,  $kl$ , and  $mn$  as shown in Fig. 6. It follows from the previous analysis in this section that dimers on these three bonds are indeed all pairwise uncorrelated. However, it is easy to see that if there is a dimer on both  $ij$  and  $kl$ , there must also be a dimer on  $mn$ . Thus  $p(ij, kl, mn) = p(ij)p(kl) = 1/16$  in this case. This result is also found from the fermionic approach, using that<sup>51</sup>

$$\langle n_{ij} n_{kl} n_{mn} \rangle = -\langle \psi_i \psi_j \psi_k \psi_l \psi_m \psi_n \rangle \quad (35)$$

which is then evaluated using Wick's theorem (Eq. (35) can be derived in the same way as Eqs. (28) and (32)). Alternatively, one can use the arrow representation. The imprint of spent arrows and constraints for  $p(ij, kl, mn)$  is shown in Fig. 6. The fact that this is also the imprint for  $p(ij, kl)$  shows that  $p(ij, kl, mn) = p(ij, kl)$ . From this figure one sees that  $\Delta\mathcal{N}_a = -14$  and  $\Delta\mathcal{N}_c = -10$ , and thus  $p(ij, kl, mn) = 2^{-14-(-10)} = 1/16$ .

## VIII. VISON CORRELATIONS

The excited-state manifold corresponding to the lowest excitation energy of the QDM Hamiltonian (3) is spanned by states that have eigenvalue  $-1$  for  $\hat{\sigma}^x(D)$  on two of the dodecagons and  $+1$  for all the others. The two localized  $\sigma^x(D) = -1$  excitations are called (point) visons.

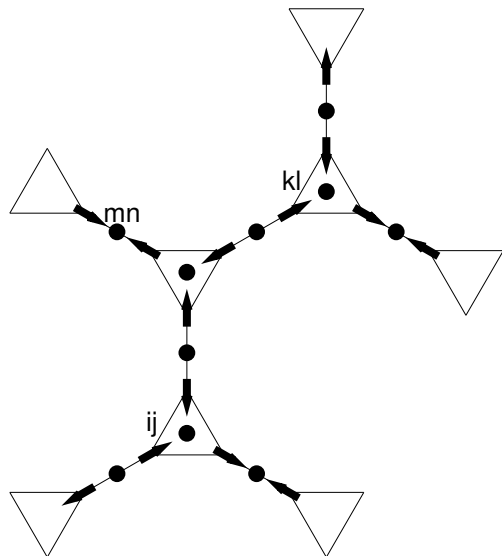


FIG. 6: Imprint of spent arrows and constraints for  $p(ij, kl, mn)$  where the three bonds  $ij$ ,  $kl$ , and  $mn$  are as shown. This imprint is the same as that for  $p(ij, kl)$ . It has  $\Delta\mathcal{N}_a = -14$  and  $\Delta\mathcal{N}_c = -10$ , giving  $p(ij, kl, mn) = p(ij, kl) = 1/16$ .

A vison can thus be labeled by the center of the hosting dodecagon. Let us find an expression for the state  $|\Psi_{I,J}\rangle$  (in a given topological sector) with visons at the dodecagon sites  $I$  and  $J$  (we use capital letters for sites on the dual lattice; the dodecagon centers form a subset of all dual lattice sites). The reasoning is analogous to the one used for the kagome lattice.<sup>19</sup> Consider a path  $\Gamma$  on the dual lattice that connects sites  $I$  and  $J$ , as shown in Fig. 7. For an arbitrary dimer covering  $|c\rangle$ , let the operator  $\hat{N}_\Gamma$  count the number of dimers  $N_\Gamma(c)$  on the bonds intersected by  $\Gamma$ . Then the operator  $(-1)^{\hat{N}_\Gamma}$  measures the associated parity, i.e. whether  $N_\Gamma(c)$  is even or odd. The dimer configuration around a dodecagon  $D$  corresponds to one of the 32 even-length loops around the dodecagon having an alternation of bonds with/without a dimer (cf. the discussion around Eq. (1)). As  $\hat{\sigma}^x(D)$  shifts the dimers by one bond along this loop, it can be seen that  $\hat{\sigma}^x(D)$  conserves the parity if  $\Gamma$  crosses the loop an even number of times, and flips the parity if  $\Gamma$  crosses the loop an odd number of times. The latter case is only realized if  $D$  is one of the endpoints  $I$  or  $J$  of  $\Gamma$ . Thus  $\hat{\sigma}^x(D)(-1)^{\hat{N}_\Gamma} = (-1)^{\hat{N}_\Gamma} \hat{\sigma}^x(D)$  if  $D \neq I, J$  and  $\hat{\sigma}^x(D)(-1)^{\hat{N}_\Gamma} = -(-1)^{\hat{N}_\Gamma} \hat{\sigma}^x(D)$  if  $D = I, J$ . It follows that the two-vison state we are looking for is given by  $|\Psi_{I,J}\rangle \equiv (-1)^{\hat{N}_\Gamma} |\text{RK}\rangle$  (here  $|\text{RK}\rangle$  is the Rokhsar-Kivelson ground state in the given topological sector) since it satisfies  $\hat{\sigma}^x(D)|\Psi_{I,J}\rangle = |\Psi_{I,J}\rangle$  for  $D \neq I, J$  and  $\hat{\sigma}^x(D)|\Psi_{I,J}\rangle = -|\Psi_{I,J}\rangle$  for  $D = I, J$ . The vison-vison correlation function is equal to (the absolute value of)

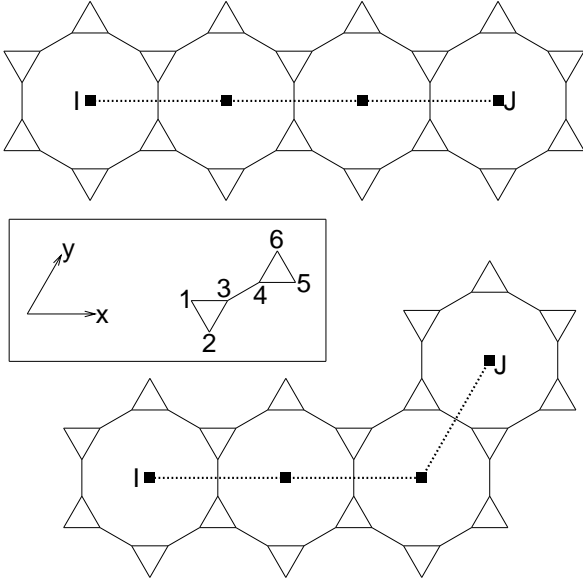


FIG. 7: Two examples (top and bottom) of a pair of visons on the star lattice. The two visons are located at the dodecagons whose centers are sites  $I$  and  $J$  on the dual lattice. A path  $\Gamma$  on the dual lattice (dotted line) connects the two vison sites. The vison-vison correlation function is equal to  $|f_e - f_o|$  where  $f_e$  ( $f_o$ ) is the fraction of all dimer coverings that has an even (odd) number of dimers on the  $n$  bonds intersected by  $\Gamma$ . The top figure is an example of the case considered in Sec. VIII A, with  $n (= n_x) = 3$ . The bottom figure is an example of the case considered in Sec. VIII B, with  $n_x = 2$ ,  $n_y = 1$  and  $n = 3$ . The inset shows the axes and unit cell in Fig. 3 translated to this figure.

the ground-state expectation value of  $(-1)^{\hat{N}_\Gamma}$ ,

$$v(I, J) \equiv |\langle \text{RK} | (-1)^{\hat{N}_\Gamma} | \text{RK} \rangle|. \quad (36)$$

Clearly  $v(I, J) = 0$  since it is the overlap of  $|\text{RK}\rangle$  and  $|\Psi_{I,J}\rangle$  which are eigenstates of the Hamiltonian with different eigenvalues. As  $(-1)^{\hat{N}_\Gamma}$  is diagonal in the dimer

basis,  $v(I, J)$  can alternatively be expressed as the correlation function

$$v(I, J) = | \langle (-1)^{\hat{N}_\Gamma} \rangle | \quad (37)$$

in the classical dimer problem.<sup>2,50,53</sup> It is instructive to rederive the vanishing of  $v(I, J)$  from Eq. (37), which is what we consider in the remainder of this section.

### A. Fermionic approach

By changing the signs of the matrix elements  $A_{ij} = -A_{ji}$  for bonds  $ij$  intersected by  $\Gamma$  (which corresponds to reversing the direction of the Kasteleyn arrows on these bonds), a dimer covering  $|c\rangle$  is counted with the sign  $(-1)^{N_\Gamma(c)}$  as required by Eq. (37). In the fermionic formulation of this expectation value, these sign changes are implemented by multiplying  $\exp(-S)$  by a compensating factor in the form of the “string”  $\prod_{(ij) \in \Gamma} \exp(2\psi_i A_{ij} \psi_j) = \prod_{(ij) \in \Gamma} (1 + 2\psi_i A_{ij} \psi_j)$ , where the product runs over all bonds intersected by  $\Gamma$ . Thus the vison-vison correlation function involves the expectation value of this string,

$$v(I, J) = \left| \left\langle \prod_{(ij) \in \Gamma} (1 + 2\psi_i A_{ij} \psi_j) \right\rangle \right|. \quad (38)$$

We may choose  $\Gamma$  to only visit dodecagon sites, so that all bonds intersected are of the linking bond type.

As an example of the evaluation of Eq. (38) we will consider the simple case shown in Fig. 7(top), where  $I$  and  $J$  have the same  $y$  coordinate and are separated by a distance  $n$ , so that  $\Gamma$  can be taken as a straight line of length  $n$  along the  $x$  axis. Thus  $\Gamma$  intersects  $n$  linking bonds. Let  $I = (X, Y)$  and  $J = (X + n, Y)$  where  $(X, Y) = (x + 1/2, y + 1/2)$ . Then  $v(I, J) = v(X, Y; X + n, Y) \equiv |\tilde{v}(n)|$  where  $\tilde{v}(n)$  is the expectation value of the string. A direct evaluation of Eq. (38) gives  $\tilde{v}(1) = \tilde{v}(2) = 0$ . For  $n \geq 3$  we write

$$\tilde{v}(n) = \left\langle \prod_{\ell=1}^n (1 + 2\psi_{x+\ell, y, 6} \psi_{x+\ell, y+1, 2}) \right\rangle = \tilde{v}(n-1) + 2 \left\langle \left[ \prod_{\ell=1}^{n-1} (1 + 2\psi_{x+\ell, y, 6} \psi_{x+\ell, y+1, 2}) \right] \psi_{x+n, y, 6} \psi_{x+n, y+1, 2} \right\rangle. \quad (39)$$

Using Wick’s theorem, the last expectation value is the sum of  $\tilde{v}(n-1) \langle \psi_{x+n, y, 6} \psi_{x+n, y+1, 2} \rangle$  and

$$\left\langle \left[ \prod_{\ell=1}^{n-2} (1 + 2\psi_{x+\ell, y, 6} \psi_{x+\ell, y+1, 2}) \right] (1 + 2\psi_{x+n-1, y, 6} \psi_{x+n-1, y+1, 2}) \psi_{x+n, y, 6} \psi_{x+n, y+1, 2} \right\rangle_{\text{ext}} \quad (40)$$

where the subscript “ext” (external) means that when evaluating this expression using Wick’s theorem, the last two Grassmann variables (GV’s)  $\psi_{x+n, y, 6}$  and  $\psi_{x+n, y+1, 2}$  should not be paired with each other. Because of Eq. (25) any pairings between GV’s whose  $x$  coordinates differ by 2 or more will vanish. It follows that the contribution to (40) from the first term in  $1 + 2\psi_{x+n-1, y, 6} \psi_{x+n-1, y+1, 2}$  will vanish. Furthermore, the only non-vanishing pairings of

$\psi_{x+n,y,6}$  and  $\psi_{x+n,y+1,2}$  are with the GV's  $\psi_{x+n-1,y,6}$  and  $\psi_{x+n-1,y+1,2}$  of the neighboring bond. Thus (40) is equal to  $2\tilde{v}(n-2)\langle\psi_{x+n-1,y,6}\psi_{x+n-1,y+1,2}\psi_{x+n,y,6}\psi_{x+n,y+1,2}\rangle_{\text{ext}}$ , so that

$$\begin{aligned} \tilde{v}(n) &= \tilde{v}(n-1)[1 + 2\langle\psi_{x+n,y,6}\psi_{x+n,y+1,2}\rangle] \\ &+ 4\tilde{v}(n-2)[\langle\psi_{x+n-1,y,6}\psi_{x+n,y+1,2}\rangle\langle\psi_{x+n-1,y+1,2}\psi_{x+n,y,6}\rangle - \langle\psi_{x+n-1,y,6}\psi_{x+n,y,6}\rangle\langle\psi_{x+n-1,y+1,2}\psi_{x+n,y+1,2}\rangle] \end{aligned} \quad (41)$$

The coefficients of  $\tilde{v}(n-1)$  and  $\tilde{v}(n-2)$  in this expression vanish, so  $\tilde{v}(n) = 0$  also for  $n \geq 3$ . (In fact, we may use Eq. (41) to conclude that  $\tilde{v}(n) = 0$  even without evaluating these coefficients, as it follows from an induction proof, using  $\tilde{v}(1) = \tilde{v}(2) = 0$ ). Thus  $v(X, Y; X+n, Y) = |\tilde{v}(n)| = 0$  for all  $n$ .

## B. Arrow approach

In this subsection we will use arguments based on the arrow representation to consider the vison-vison correlation function  $v(X, Y; X+n_x, Y+n_y)$  with both  $n_x$  and  $n_y$  arbitrary. In this case  $\Gamma$  can be taken to be made up of two straight line segments of length  $|n_x|$  in the  $x$  direction and length  $|n_y|$  in the  $y$  direction. An example with  $n_x$  and  $n_y$  positive is shown in Fig. 7(bottom). Again, we note that all the bonds intersected by  $\Gamma$  are of the linking bond type. The fraction of dimer coverings that has a specific distribution of dimers on the  $n$  intersected bonds ( $n = |n_x| + |n_y|$ ) is equal to  $2^{-n}$ . This is because the presence or absence of a dimer on a linking bond has a probability  $p_t = 1 - p_t = 1/2$ , and dimers can be distributed independently on the linking bonds intersected by  $\Gamma$ . This independence can be seen by laying down arrows corresponding to a particular dimer distribution on these linking bonds; the bonds will contribute additively to  $\Delta\mathcal{N}_a - \Delta\mathcal{N}_c$ . (Note that for a linking bond, not only the presence, but also the absence of a dimer, is associated with a definite configuration of the arrows on the two sites connected by that linking bond.) Distributing dimers on the intersected bonds in all possible ways should generate all dimer coverings. To check that our arguments produce this result, we note that the number of ways to lay down  $k$  dimers on  $n$  bonds is  $\binom{n}{k}$  and thus the total fraction of configurations generated this way is  $2^{-n} \sum_{k=0}^n \binom{n}{k} = 1$  as expected. Furthermore, the fraction of configurations  $f_e$  and  $f_o$  with an even and odd number of intersected dimers, respectively, is given by

$$f_e = 2^{-n} \sum_{\substack{k \text{ even} \\ 0 \leq k \leq n}} \binom{n}{k} = \frac{1}{2}, \quad (42)$$

$$f_o = 2^{-n} \sum_{\substack{k \text{ odd} \\ 0 \leq k \leq n}} \binom{n}{k} = \frac{1}{2}. \quad (43)$$

Since the vison-vison correlation function (37) can be written  $|f_e - f_o|$ , Eqs. (42)-(43) imply that it vanishes.

## IX. MONOMER CORRELATIONS

All properties considered so far have been for a system in which every site is touched by exactly one dimer. A different but closely related problem involves a lattice in which some sites are occupied by monomers, meaning that those sites cannot be touched by a dimer. In this section we consider a system with two monomers. We will be interested in the monomer-monomer correlation function, defined as

$$m(i, j) = \frac{\mathcal{Z}_{mm}(i, j)}{\mathcal{Z}} \quad (44)$$

where, for the CDM with equal dimer weights,  $\mathcal{Z}_{mm}(i, j)$  is the number of possible dimer coverings when the system has monomers at sites  $i$  and  $j$ ,<sup>54</sup> and  $\mathcal{Z}$  is the same as before, i.e. the number of dimer coverings for the system in the absence of monomers. More generally, if not all dimer weights are equal, the two quantities in Eq. (44) are the generating functions for the system with and without the monomers.<sup>8</sup>

The monomers in a CDM can be characterized as confined or deconfined. A deconfined phase is characterized by a nonzero value of  $m(i, j)$  in the limit of infinite monomer separation  $|i - j| \rightarrow \infty$ , while in a confined phase  $m(i, j)$  goes to zero in this limit. Using Fisher's mapping,<sup>10</sup> Moessner and Sondhi<sup>11</sup> were able to show that the star-lattice CDM has a phase transition as a function of the dimer weights in which monomers are confined in one phase and deconfined in the other. They did this by relating certain sums of four monomer-monomer correlation functions to a spin-spin correlation function in the square-lattice Ising model. This approach does however not allow one to deduce  $m(i, j)$  itself.

In this section we calculate the monomer-monomer correlation function for a star-lattice CDM with equal dimer weights. We find that  $m(i, j) = 1/4$  for all possible choices of the monomer sites  $i$  and  $j$  (with  $i \neq j$ ) except when  $i$  and  $j$  are connected by a linking bond, in which case  $m(i, j) = 1/2$ . Thus the monomers are deconfined in this case. As we discuss in Sec. IX C, these results are consistent with the analysis in Ref. 11.

### A. Fermionic approach

The lattice graph of the system with monomers at sites  $i$  and  $j$  differs from the original lattice graph in that sites  $i$  and  $j$ , as well as all bonds connected to them, are removed. This modified lattice graph is still planar so the

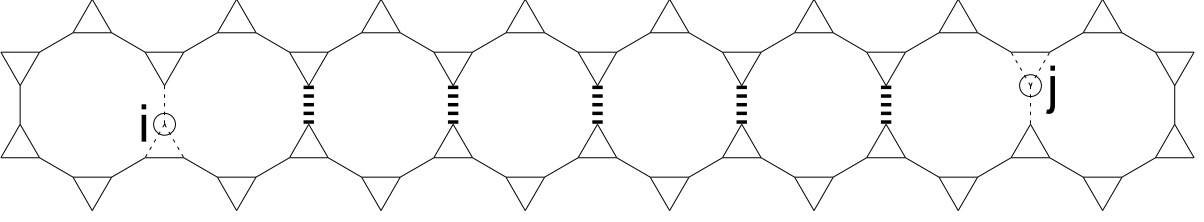


FIG. 8: A particular case of the two-monomer system for which Eq. (47) for the monomer-monomer correlation function  $m(i, j)$  is evaluated in the text. The two monomers are located at sites  $i$  and  $j$  of the original lattice (shown as open circles). In this figure,  $i = (x, y, 6)$  and  $j = (x+n, y+1, 2)$  with  $n = 6$  (cf. the site labeling conventions in Fig. 3 and the inset in Fig. 7). The removed bonds connected to these sites are shown as dashed lines. The bonds whose Kasteleyn arrows are reversed in this fermionic calculation are shown as thick dotted lines.

Pfaffian method can again be applied.<sup>2,8</sup> Due to the bond removals, the question of signs for the Kasteleyn matrix elements needs to be readdressed. Let us consider the generic situation when the monomers are sufficiently far apart that they sit on separate faces; for the star lattice each of the faces hosting a monomer has 21 bonds along its perimeter. Consider a “path of faces” connecting the two monomer sites, with all but the two end faces on this path being dodecagons. Neighboring faces along this path then share one linking bond. It can be seen that the original choice of Kasteleyn arrows violates the clockwise-odd sign rule around the two end faces hosting the monomers, while the sign rule is respected on the other faces on the path. A valid choice of signs is then obtained by reversing the Kasteleyn arrows on each of the single bonds shared by neighboring faces along the path, such that one arrow is reversed around each of the two end faces, and two arrows are reversed around each of the interior faces.<sup>2,8</sup> An example (which we will return to below) is shown in Fig. 8.

We now give a derivation of the general expression for  $m(i, j)$  in the fermionic approach (see also Ref. 2). We have  $Z_{mm}(i, j)/Z = |Z_{mm}(i, j)/Z|$  where, by analogy with the original lattice graph,  $Z_{mm}(i, j)$  is given by

$$Z_{mm}(i, j) = \int \mathcal{D}\psi_{i,j} \exp(-S_{i,j}). \quad (45)$$

Here  $\int \mathcal{D}\psi_{i,j} = \int \prod_l' d\psi_l$  and  $S_{i,j} = \frac{1}{2} \sum_{k,l}' \psi_k \bar{A}_{kl} \psi_l$ , where  $\bar{A}$  is the modified Kasteleyn matrix (i.e. with the necessary sign changes) and the prime on the product and sum means that the Grassmann variables for sites  $i$  and  $j$  are excluded. To express  $Z_{mm}(i, j)$  as an expectation value with respect to the original lattice graph, we use that  $\exp(-S_{i,j})$  can be written as

$$\begin{aligned} & \exp\left(\psi_i \sum_k A_{ik} \psi_k\right) \exp\left(\psi_j \sum_l A_{jl} \psi_l\right) \exp(-\psi_i A_{ij} \psi_j) \\ & \times \left( \prod_{(mn) \in \Lambda} (1 + 2\psi_m A_{mn} \psi_n) \right) \exp(-S) \end{aligned} \quad (46)$$

Here the fourth factor that takes care of the sign reversals is a “string” of the same type encountered in the fermionic calculation of the vison-vison correlation function in Sec. VIII A; the product again goes over the bonds whose Kasteleyn arrows are reversed. Furthermore,  $\int \mathcal{D}\psi_{i,j} = \int \mathcal{D}\psi \psi_i \psi_j$  (up to a possible sign difference). The presence of  $\psi_i \psi_j$  here implies that when (46) is inserted into (45), the first three factors in (46) can be replaced by 1, as the omitted terms will give no contribution to  $Z_{mm}(i, j)$  owing to  $\psi_i^2 = \psi_j^2 = 0$ . Thus<sup>2</sup>

$$m(i, j) = \left\langle \psi_i \left( \prod_{(kl) \in \Lambda} (1 + 2\psi_k A_{kl} \psi_l) \right) \psi_j \right\rangle. \quad (47)$$

We will now evaluate Eq. (47) for the case that the left (right) monomer is at site  $i$  ( $j$ ) where  $i = (x, y, 6)$  or  $(x, y+1, 2)$  and  $j = (x+n, y, 6)$  or  $(x+n, y+1, 2)$ , where  $n > 0$ . Thus the  $x$  coordinates of the two monomers differ by  $n$ . The directions of the Kasteleyn arrows on the  $n-1$  vertical linking bonds between  $i$  and  $j$  are reversed. The particular case  $i = (x, y, 6)$ ,  $j = (x+n, y+1, 2)$  with  $n = 6$  is illustrated in Fig. 8. Consider the expression

$$\langle \psi_i \left[ \prod_{\ell=1}^{n-1} (1 + 2\psi_{x+\ell, y, 6} \psi_{x+\ell, y+1, 2}) \right] \psi_j \rangle \quad (48)$$

whose absolute value is  $m(i, j)$ . When evaluating this using Wick’s theorem, all terms involving a 1 from one or more of the factors  $(1 + 2\psi_{x+\ell, y, 6} \psi_{x+\ell, y+1, 2})$  will give zero contribution due to the property (25) of the Green function. Hence the only surviving term in (48) is the one with all  $2n$  Grassmann variables present,

$$\langle \psi_i \left[ \prod_{\ell=1}^{n-1} 2\psi_{x+\ell, y, 6} \psi_{x+\ell, y+1, 2} \right] \psi_j \rangle \equiv \tilde{m}_{\alpha\beta}(n). \quad (49)$$

Here  $\alpha$  and  $\beta$  are the intra-cell coordinates of sites  $i$  and  $j$  respectively, i.e.  $\alpha$  and  $\beta$  can take the values 2 and 6. We find  $\tilde{m}_{62}(1) = \tilde{m}_{66}(1) = -\tilde{m}_{22}(1) = -\tilde{m}_{26}(1) = 1/4$ ,

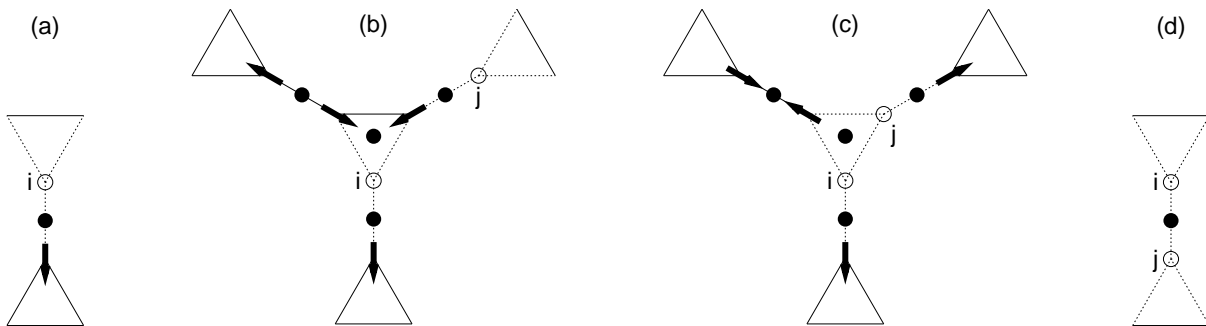


FIG. 9: Arrow calculation of monomer-monomer correlation function. (a) Imprint (set of spent arrows and constraints) for a single monomer located at site  $i$ . The open circle denotes the removed arrow on the site. The filled circle denotes the spent constraint. (b), (c), and (d): Imprints for some two-monomer configurations. For each of these,  $m(i, j)$  can be found by inserting the number of spent arrows and constraints into Eq. (30).

while for  $n \geq 2$ ,

$$\begin{aligned} \tilde{m}_{\alpha\beta}(n) &= 2[\tilde{m}_{\alpha,6}(n-1)\langle\psi_{x+n-1,y+1,2}\psi_j\rangle \\ &\quad - \tilde{m}_{\alpha,2}(n-1)\langle\psi_{x+n-1,y,6}\psi_j\rangle] \\ &= -\frac{1}{2}[\tilde{m}_{\alpha,6}(n-1) + \tilde{m}_{\alpha,2}(n-1)]. \end{aligned} \quad (50)$$

Thus  $\tilde{m}_{\alpha\beta}(n)$  is independent of  $\beta$ . Defining  $\tilde{m}_\alpha(n) \equiv \tilde{m}_{\alpha\beta}(n)$ , we have

$$\tilde{m}_\alpha(n) = -\tilde{m}_\alpha(n-1) \quad (n \geq 2), \quad (51)$$

with  $\tilde{m}_6(1) = -\tilde{m}_2(1) = 1/4$ . It follows that the monomer-monomer correlation function  $m(i, j) = |\tilde{m}_\alpha(n)| = 1/4$  for any  $n$ , including the limit  $n \rightarrow \infty$ .

We note that both the monomer-monomer correlation function considered here and the vison-vison correlation function considered in Sec. VIII contain a “string” in the fermionic formulation. This string causes the number of pairings from Wick’s theorem to grow exponentially with the vison/monomer separation. However, in both cases the property (25) comes to the rescue by making most of these pairings vanish. As a result the calculations are analytically tractable regardless of the vison/monomer separation. This should be contrasted with the situation for the triangular-lattice CDM discussed in Ref. 2, for which the exponential growth of the number of pairings made the fermionic calculation of the monomer-monomer correlation function prohibitively difficult for all but the smallest values of the monomer-monomer separation. Instead this calculation was there carried out with a determinant formulation first used by Fisher and Stephenson for the square lattice.<sup>8</sup> This determinant formulation was also used for the Pfaffian calculation of the monomer-monomer correlation function of the kagome lattice CDM recently reported in Ref. 26.

Despite the essential simplifications resulting from Eq. (25), the fermionic approach to the monomer-monomer correlation function is still less economical and less intuitive than the arrow approach to be discussed below. For

some cases of small monomer separation, the fermionic calculation of  $m(i, j)$  on the star lattice also has an additional technical complication: the modified lattice graph has *cut points*,<sup>55</sup> the existence of which violates the conditions for the explicit proof of the clockwise-odd rule given in Ref. 1. While this complication can be dealt with (the Pfaffian method can be used also for a graph with cut points<sup>1</sup>), and one reassuringly finds<sup>56</sup> the same result for  $m(i, j)$  as obtained from the arrow representation, the arrow derivation is much simpler, and therefore we do not discuss these fermionic calculations further here.

## B. Arrow approach

The monomer-monomer correlation function (44) is yet another example of a ratio of the general type discussed in Sec. VIB that can be calculated using the arrow approach. Thus we must again identify the appropriate values of  $\Delta\mathcal{N}_a$  and  $\Delta\mathcal{N}_c$  in Eq. (30). Let us start by looking at the situation when the two monomer sites  $i$  and  $j$  are far apart. Consider the monomer at one of the sites, say  $i$ . Its contributions to  $\Delta\mathcal{N}_a$  and  $\Delta\mathcal{N}_c$  are  $-2$  and  $-1$ , respectively. Here, the two spent arrow ( $Z_2$ ) degrees of freedom are the (removed) arrow on  $i$  and the arrow on the site at the opposite end of the (removed) linking bond that  $i$  was originally one endpoint of; in the presence of the monomer this latter arrow must point into the neighboring triangle. Furthermore, the spent constraint contributing to  $\Delta\mathcal{N}_c$  is the constraint on this (removed) linking bond.<sup>57</sup> The set of spent arrows and constraints for an individual monomer will be referred to as the monomer *imprint* (see Fig. 9(a)). When the two monomers are far apart their contributions to  $\Delta\mathcal{N}_a$  and  $\Delta\mathcal{N}_c$  simply add, giving  $m(i, j) = 2^{2(-2-(-1))} = 1/4$ . This result is of course also valid as the separation between the monomers is increased to infinity, and is independent of the relative orientation between the underlying lattice graph and the vector connecting the two monomers.

Next, let us analyze what happens when the two monomers are moved closer to each other. As long as the monomers are not too close, the situation remains the same: The two monomer imprints do not overlap, nor do they touch the same triangle, so  $\Delta\mathcal{N}_a$  and  $\Delta\mathcal{N}_c$  are given by the sum of the separate contributions from each monomer. Thus  $\Delta\mathcal{N}_a - \Delta\mathcal{N}_c$  is also additive, giving  $m(i, j) = 1/4$ . Only when the two monomers get so close that their relative positions are as shown in Fig. 9(b) do their respective imprints touch the same triangle (the middle one in the figure). Now  $\Delta\mathcal{N}_a$  and  $\Delta\mathcal{N}_c$  are no longer additive, but as the additional contributions to  $\Delta\mathcal{N}_a$  and  $\Delta\mathcal{N}_c$  are equal,  $\Delta\mathcal{N}_a - \Delta\mathcal{N}_c$  is still additive, so again  $m(i, j) = 1/4$ . This continues to hold when  $j$  is moved even closer so that  $i$  and  $j$  are connected by a triangle bond, as shown in Fig. 9(c). If, on the other hand,  $j$  approaches  $i$  from the side of  $i$ 's linking bond, they will finally end up being connected by this linking bond, as shown in Fig. 9(d). In this case  $\Delta\mathcal{N}_a = -2$  and  $\Delta\mathcal{N}_c = -1$  so  $m(i, j) = 1/2$ .

### C. Connection to spin-spin correlations in the square-lattice Ising model

As shown by Moessner and Sondhi<sup>11</sup> (see also Ref. 34), by using Fisher's mapping<sup>10</sup> between the ferromagnetic Ising model on the square lattice and the classical dimer model on the star lattice, the spin-spin correlation function for the spin model can be related to a sum of monomer-monomer correlation functions for the dimer model. In our notation, this relation can be written

$$\langle S(x, y)S(x', y') \rangle = \sum_{\alpha, \alpha'=3,4} m(x, y, \alpha; x', y', \alpha'). \quad (52)$$

Here  $S(x, y)$  is the Ising spin located at position  $(x, y)$  of the square lattice. In Fisher's mapping, the dimer weights on the bonds corresponding to the original square lattice (see Fig. 3(left)) are  $1/\tanh(\beta J_{ij})$  (where  $\beta$  is the inverse temperature and  $J_{ij}$  is the ferromagnetic Ising exchange parameter) while the dimer weights on the bonds internal to the unit cell (see Fig. 3(right)) are 1. The relation (52) implies that the phase transition of the Ising model between states with unbroken/broken spin rotation symmetry maps onto a confinement-deconfinement transition in the dimer model.<sup>11</sup> The equal-weight dimer model considered in this paper is obtained in the zero-temperature limit  $\beta \rightarrow \infty$  of the Ising model, in which case the spins are perfectly ordered so the lhs of Eq. (52) equals 1. Let us use our results for  $m(i, j)$  to evaluate the rhs of Eq. (52) for this case. When  $(x, y) \neq (x', y')$  all four monomer-monomer correlation functions in (52) equal  $1/4$ , so the rhs is  $4 \cdot 1/4 = 1$ . On the other hand, when  $(x, y) = (x', y')$  the two monomer-monomer correlation functions with  $\alpha = \alpha'$  vanish since with both monomers on the same site, no dimer coverings are possible (as there is an odd number of sites left to form dimers). As the two remaining terms have  $m(i, j) = 1/2$ ,

the sum is now  $2 \cdot 0 + 2 \cdot 1/2 = 1$ . Thus our results for  $m(i, j)$  do indeed satisfy Eq. (52).

## X. COMPARISON WITH DIMERS ON THE KAGOME LATTICE

As briefly summarized in Sec. I, dimers on the kagome lattice have very interesting properties.<sup>19,21,22,23,24,26,49</sup> One may consider the existence of an arrow representation of dimer coverings on the kagome lattice<sup>19,21,22</sup> to be a "fundamental" property, in the sense that the other properties can be derived from it. Alternatively, using the Pfaffian method, the "fundamental" property is that the Green function of the kagome lattice vanishes beyond a very short distance.<sup>23,24</sup>

As shown in this paper, the properties of dimers on the star lattice closely parallel those on the kagome lattice. Again, the most fundamental properties, from which all others can be shown to follow, are the existence of an arrow representation, or, alternatively, the Green function satisfying Eq. (25). (Note that the number of dimer coverings  $\mathcal{Z}$  considered in Sec. IV is also related to the Green function:  $\mathcal{Z} \sim \sqrt{\det A} = 1/\sqrt{\det G}$ .) In the following we will discuss the similarities and connections between dimers on the star and kagome lattices in some more detail. We emphasize that, unless explicitly stated otherwise, all comparisons in this section between classical dimers on these two lattices (including those made above) are for the case when all dimers have equal weights, which is the case we have considered in this paper. At the end we will briefly comment on the star-lattice CDM for unequal dimer weights, whose properties are more conventional.

First, however, let us note a close relationship between the star and kagome lattices themselves.<sup>30,35,36,37</sup> These two lattices can be regarded as "expanded" and "reduced" versions of each other, in the following sense: Starting from the kagome lattice with  $N_k$  sites, touching triangles can be separated by splitting their common site into two sites connected by a new bond. The resulting "expanded" lattice is a star lattice with  $N_s = 2N_k$  sites (the new bonds are the linking bonds of the star lattice). Reversely, starting from a star lattice with  $N_s$  sites, the linking bonds can be shrunk to zero length and the two sites at its ends merged into one. The resulting "reduced" lattice is a kagome lattice with half as many sites.

*The number of dimer coverings.* For a kagome lattice of  $N_k$  sites embedded on a closed surface the number of dimer coverings is<sup>19,21,22,49,58</sup>  $\mathcal{Z}_k(N_k) = 2^{N_k/3+1}$ . As shown in Sec. IV A, the corresponding result for a star lattice with  $N_s$  sites is  $\mathcal{Z}_s(N_s) = 2^{N_s/6+1}$ . Thus the kagome and star lattices that are each other's reduced/expanded lattices with  $N_s = 2N_k$  have exactly the same number of dimer coverings:

$$\mathcal{Z}_s(N_s) = \mathcal{Z}_k(N_k). \quad (53)$$



A related special property of the kagome and star lattice is that they have very simple expressions for the entropy per site/dimer (a simple rational number times  $\log 2$ ), in contrast to e.g. the square, honeycomb and triangular lattice.<sup>3</sup> The squagome<sup>19,22</sup> and triangular-kagome lattice<sup>26</sup> also have this property; we will comment more on this in Sec. XI B.

A consequence of Eq. (53) is that the Hilbert spaces of QDMs defined on the kagome/star lattices that are reduced/expanded versions of each other have the same dimension. One can therefore construct one-to-one mappings between the basis states (dimer coverings) in these Hilbert spaces. One possible mapping is as follows: Pick an arbitrary dimer covering  $|c_k\rangle$  on the kagome lattice and map this to an arbitrary dimer covering  $|c_s\rangle$  on the star lattice. Then map the dimer covering  $\prod \hat{\sigma}^x(H)|c_k\rangle$  on the kagome lattice to the dimer covering  $\prod \hat{\sigma}^x(D)|c_s\rangle$ . Here the product runs over some set of hexagons in the kagome case and over the associated set of dodecagons in the star lattice case (a given hexagon in the kagome lattice is associated with a unique dodecagon in the star lattice by the “extension/reduction” procedure described earlier). In this way one gets a one-to-one mapping between dimer coverings in given topological sectors on the two lattices. This mapping is particularly “natural” from the point of view of the QDM Hamiltonian (3) and its kagome analogue considered in Ref. 19, as they are given by a sum of  $\hat{\sigma}^x$  operators on all hexagons/dodecagons.

*Dimer-dimer correlations.* On both the kagome and star lattice a dimer is uncorrelated with any dimer further away than on a neighboring triangle. For the kagome lattice this means that a dimer is correlated with dimers that are up to three bonds away,<sup>19,23,24</sup> while for the star lattice, as shown in Sec. VII, dimers on triangle bonds are correlated with dimers up to four bonds away, while dimers on linking bonds are correlated with dimers that are only up to two bonds away (in fact, only with the triangle-bond subset of these, as a linking bond dimer is uncorrelated even with dimers on the nearest linking bonds that are only two bonds away). Furthermore, comparing Fig. 5(a) with the corresponding figure for the kagome lattice (the latter can be constructed from the results in Ref. 24, or calculated from the arrow representation), one finds that the numbers on the triangle in the middle are identical while those on the three outer triangles have the same magnitude but opposite sign (the linking bonds are of course not there in the kagome lattice figure).

*Vison-vison correlations.* The vison-vison correlation function  $v(I, J)$  vanishes for both lattices (here  $I$  and  $J$  are hexagon/dodecagon sites, respectively). In both cases this is most easily seen from the fact that, as discussed in Sec. VIII, the state with visons at  $I$  and  $J$  is an eigenstate of the QDM Hamiltonian, and the absolute value of the overlap between this two-vison excited state and the ground state is just the vison-vison correlation function.

*Monomer-monomer correlations.* The monomer-

monomer correlation function  $m(i, j)$  on the kagome lattice equals  $1/4$  for all monomer sites  $i$  and  $j$ .<sup>25,26</sup> As shown in Sec. IX, the same result holds for the star lattice, with one exception: when  $i$  and  $j$  are connected by a linking bond,  $m(i, j) = 1/2$ .

Finally, we note that the result (25) for the star-lattice Green function is limited to the case of equal dimer weights that we have considered in this paper. As a consequence, the very special properties of the star-lattice CDM for equal dimer weights do not carry over to unequal dimer weights. In contrast, the special properties of dimers on the kagome lattice are more robust, as the result (25) continues to hold also if the dimer weight is allowed to depend on the orientation of the bond.<sup>23,24</sup>

## XI. GENERAL FISHER LATTICES AND THEIR “REDUCED” LATTICES

It is interesting to ask whether the results obtained here for the star lattice can be generalized to other lattices. A natural class of lattices to consider in this respect are those hosting the dimers in Fisher’s mapping from an Ising model to a dimer problem,<sup>10</sup> of which the star lattice is one particular example. Any such “terminal” lattice in Fisher’s mapping will here be referred to as a general Fisher lattice, or just Fisher lattice for short. The sites (vertices) in a general Fisher lattice can have coordination number (henceforth called degree) 1, 2, or 3. Sites of degree 3 are part of a triangle of three sites connected by bonds which we call triangle bonds. All other bonds in the Fisher lattice will be called linking bonds.

### A. Arrow representation and the number of dimer coverings for general Fisher lattices

An arrow representation of dimer coverings exists also for a general Fisher lattice. Again, the arrows are Ising degrees of freedom living on the lattice sites, and each triangle and each linking bond contribute an arrow constraint. Using the arrow representation, one can calculate various properties of dimers on general Fisher lattices, analogously to what we have done for the star lattice. As an example, we will show that the arrow representation gives the correct answer for the number of dimer coverings on an arbitrary Fisher lattice. We do this by first using Fisher’s mapping to calculate this number, and then we show that the arrow representation gives the same result.

Thus let us consider Eq. (11) in Ref. 10, which relates the Ising model partition function (defined in Fisher’s Eq. (3)) to the generating function of dimer coverings on the associated Fisher lattice. We are interested in the case of equal dimer weights, i.e.  $v_{ij} = 1$ , for which this generating function reduces to the number of dimer coverings  $\mathcal{Z}$  on the Fisher lattice. This gives (in our nota-

tion)  $\mathcal{Z}_I = 2^{N_I - N_{I,b}} \mathcal{Z}$ . Here  $\mathcal{Z}_I$  is the partition function of the Ising model and  $N_I$  and  $N_{I,b}$  are the number of sites and bonds in the lattice on which this Ising model is defined (which we will refer to as the Ising lattice). As the equal-weight case maps to the zero-temperature limit of the Ising model,  $\mathcal{Z}_I = 2$  since only the two perfectly ordered states related by time reversal contribute to  $\mathcal{Z}_I$  in this limit. Thus

$$\mathcal{Z} = 2^{N_{I,b} - N_I + 1}. \quad (54)$$

Next, let us calculate  $\mathcal{Z}$  using the arrow representation. As in Sec. IV A, we have  $\mathcal{Z} = 2^{\mathcal{N}_a - \mathcal{N}_c}$  where  $\mathcal{N}_a$  is the number of  $Z_2$  arrow degrees of freedom and  $\mathcal{N}_c$  is the number of independent arrow constraints. For a general Fisher lattice we have  $\mathcal{N}_a = N_F - N_F^{(1)}$  where  $N_F$  is the number of sites on the Fisher lattice and  $N_F^{(1)}$  is the number of sites of degree 1. The reason for subtracting  $N_F^{(1)}$  is that an arrow on a site of degree 1 has to point towards the single bond connected to the site (because the site has to be touched by a dimer) and is therefore not a  $Z_2$  degree of freedom. The number of independent arrow constraints is  $\mathcal{N}_c = N_T + N_l - 1$  where  $N_T$  is the number of triangles and  $N_l$  is the number of linking bonds in the Fisher lattice. As in Sec. IV A the term  $-1$  in  $\mathcal{N}_c$  comes about because one of the  $N_T + N_l$  constraints can be deduced from the others. We show in Appendix B 1 that

$$(N_F - N_F^{(1)}) - (N_T + N_l) = N_{I,b} - N_I \quad (55)$$

which means that the result (54) is indeed reproduced by the arrow representation. In Appendix B 1 we also show that

$$N_{I,b} - N_I = \frac{1}{6}(N_F - N_F^{(2)}) - \frac{2}{3}N_F^{(1)}. \quad (56)$$

For a general Fisher lattice we therefore have

$$\mathcal{Z} = 2^{(N_F - N_F^{(2)})/6 - 2N_F^{(1)}/3 + 1}. \quad (57)$$

For Fisher lattices with no sites of degree 1 or 2 this simplifies to

$$\mathcal{Z} = 2^{N_F/6 + 1}. \quad (58)$$

This simplification applies e.g. to the star lattice graph considered in Sec. IV A, as all its sites have degree 3; the result for  $\mathcal{Z}$  is indeed the same as found there. In Appendix B 2 we check the result (57) for some Fisher lattices with sites of degree 1 and/or 2.

### B. The “reduced” lattice of a Fisher lattice

The kagome lattice is the “reduced” lattice of the star lattice in the sense described in Sec. X. An analogous reduction procedure, consisting of shrinking the linking bonds to zero and merging all sites that come together

in this process, can be carried out for any Fisher lattice F. Unless F is trivial by not containing any triangles, the sites in the reduced lattice R so obtained have coordination number four.

As a first example, consider the Fisher lattice associated with the triangular-lattice Ising model, which can be shown to consist of triangles, octagons, and “16-gons.” The reduced Fisher lattice R is a squagome lattice.<sup>22,59</sup> This is a lattice of corner-sharing triangles and therefore has an arrow representation of its own as noted in Refs. 19,22.

As a second example, consider the kagome-lattice Ising model. The lattice E (this notation is explained in Appendix B) is then the star lattice. The Fisher lattice F is obtained by replacing each site of the star lattice with a triplet of sites connected by a triangle of additional bonds. The reduced lattice R of this Fisher lattice is the triangular-kagome lattice recently considered in Ref. 26. Although this is not a lattice of corner-sharing triangles (as its triangles also share edges), it still has an arrow representation. To see this, note that any dimer on this lattice can be uniquely associated with an “outer small” triangle. (Each “big” triangle consists of 4 small triangles: 3 outer and 1 inner). Therefore an arrow representation exists in which each arrow must point into one of the two outer small triangles that its site connects, i.e. the arrows are again  $Z_2$  variables. The fact that the inner small triangles have a different status than the outer small ones is reflected in the fact that the former triangles are not present in the Fisher lattice F but only appear after F has been reduced to R.

The number of dimer coverings on F and R are closely related, as we have already seen for the star and kagome lattice in Sec. X. The reduction of F to R involves removing one site for each linking bond, and therefore the difference  $\mathcal{N}_a - \mathcal{N}_c$  is the same in F and R, and thus so is the number of dimer coverings (cf. Eq. (53)). Since the number of sites on the two lattices are related by  $N_F = 2N_R$ , the entropy per site on R in the thermodynamic limit is, from Eq. (58), given by  $s_R = (1/3) \log 2$ , which agrees with previous calculations in the literature.<sup>19,21,22,26,49,58</sup> The fact that the entropy per site is the same for the kagome, squagome, and triangular kagome lattice can thus be understood to be a consequence of the fact that each of these lattices is the reduced lattice of a Fisher lattice for which Eq. (58) holds.

Based on the existence of the arrow representation as well as recent studies of what we have here dubbed reduced Fisher lattices,<sup>19,22,26</sup> we expect that also other properties of dimers on general Fisher lattices and their reduced lattices should in general be closely related and resemble those of the star and kagome lattice (one exception is the purely one-dimensional Fisher lattices considered in Sec. B 2).

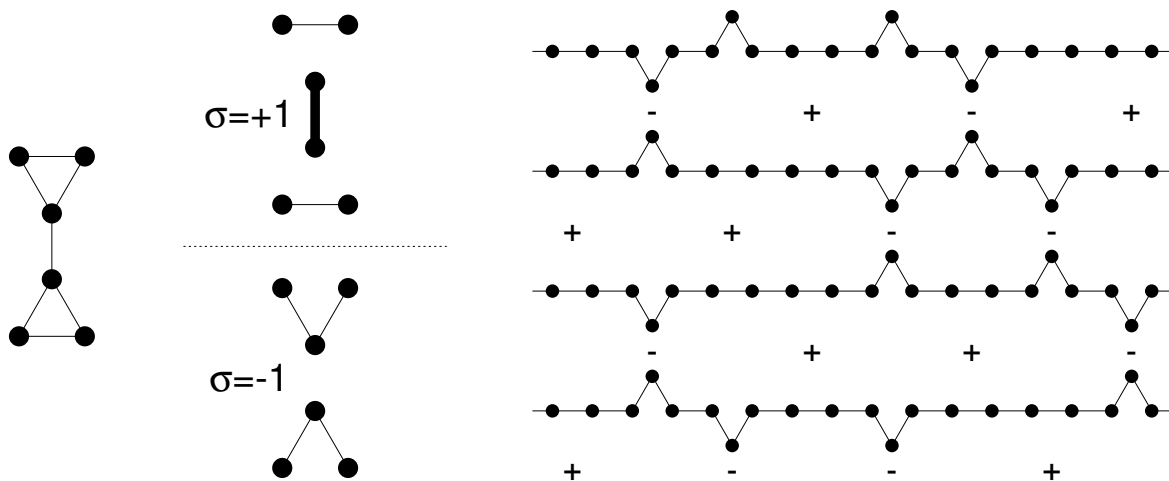


FIG. 10: In this figure filled circles represent lattice sites. Left: 6-site unit cell for the star lattice. An Ising pseudospin  $\sigma = \pm 1$  is associated with the vertical linking bond connecting the two triangles. Middle: The unit cell graph that results from deleting the bonds that, for the given value of  $\sigma$ , cannot be occupied by a dimer. (The thick line in the  $\sigma = +1$  graph is the dimer on the linking bond.) Right: The decoupled horizontal loops resulting from deleting the appropriate bonds in all unit cells for a particular pseudo-spin configuration (the pseudo-spins are shown as signs  $\pm$ ) in a system with  $L = 4$ . (For ease of drawing, the vertical dimers in the  $\sigma = +1$  unit cells are not shown and the bonds connecting different unit cells have all been made horizontal.)

## XII. FINAL REMARKS

We conclude by mentioning another lattice recently considered in the literature that also has an arrow representation. This lattice, which is a hybrid of the kagome and star lattices, is shown in Fig. 1 (right) in Ref. 11, which considered a dimer problem on this lattice. Using the arrow representation one can e.g. reproduce the result for equal-weight dimers ( $u = 1$ ) obtained in Ref. 11 with the Pfaffian method.

### Acknowledgments

We thank Grégoire Misguich and Roderich Moessner for comments on the manuscript. This research was supported by the Australian Research Council.

### APPENDIX A: AN ALTERNATIVE PSEUDO-SPIN REPRESENTATION OF DIMER COVERINGS ON THE STAR LATTICE

Recently Dhar and Chandra introduced an alternative pseudo-spin representation of dimer coverings on lattices of corner-sharing triangles.<sup>43</sup> Wu and Wang used this representation to give a derivation of the number of dimer coverings on a finite kagome lattice.<sup>49</sup> In this Appendix we generalize this pseudo-spin representation to the star lattice and use it to give an alternative simple derivation of the result (18) for the number of dimer coverings on a

finite star lattice on a torus.

Consider the star lattice as shown in Fig. 1. Here we will choose the 6-site unit cells to be oriented as shown in Fig. 10 (left panel). A unit cell will be labeled  $(k, \ell)$  where  $k = 1, \dots, K$  and  $\ell = 1, \dots, L$ . Here  $L$  is the number of horizontal rows of these unit cells and  $K$  is the number of unit cells in each such row. We will consider the star lattice graph to have a torus geometry by connecting opposite ends in the horizontal and vertical direction. The number of unit cells is  $N/6$  where  $N = 6KL$  is the total number of sites in the lattice.

We now associate an Ising pseudo-spin variable  $\sigma_{k\ell} = \pm 1$  with the vertical linking bond in unit cell  $(k, \ell)$ . We define  $\sigma_{k\ell} = +1$  ( $-1$ ) if this linking bond is occupied (not occupied) by a dimer. Let us consider how many dimer coverings are associated with a given pseudo-spin configuration  $\{\sigma_{k\ell}\}$ . One sees that for a given value of  $\sigma_{k\ell}$  some bonds in the unit cell  $(k, \ell)$  cannot be occupied by a dimer. By removing these bonds in all the unit cells one obtains a new lattice graph that consists of  $L$  disconnected horizontal closed loops of bonds. This is illustrated in Figs. 10 (middle and right panels). If all of these disconnected loops contain an even number of sites, the number of dimer coverings associated with the pseudo-spin configuration is  $2^L$ , since there are two dimer coverings for each loop. On the other hand, if some loops have an odd number of sites, no dimer coverings are possible for the given pseudo-spin configuration.

It remains to find the number of pseudo-spin configurations that are consistent with dimer coverings. To this

end, we define the variables<sup>49</sup>

$$\tau_\ell = \prod_{k=1}^K \sigma_{k\ell}, \quad \ell = 1, \dots, L. \quad (\text{A1})$$

If  $\sigma_{k\ell} = +1$  the unit cell  $(k, \ell)$  contributes 2 sites to each of the two loops above and below it, while if  $\sigma_{k\ell} = -1$  the unit cell contributes 3 sites to each of these loops. In order for the loop going between unit cell rows  $\ell$  and  $\ell+1$  to contain an even number of sites, an even number of the unit cells contributing sites to it must have pseudo-spin  $\sigma = -1$ . This constraint can be written

$$\tau_\ell \tau_{\ell+1} = 1. \quad (\text{A2})$$

There are  $L$  such constraints, one for each loop. However, only  $L-1$  of these are independent, since due to  $\sigma_{k\ell}^2 = 1$  we have

$$(\tau_1 \tau_2)(\tau_2 \tau_3) \dots (\tau_L \tau_1) = 1 \quad (\text{A3})$$

so one of the constraints can be deduced from the others. The number of pseudo-spin configurations that are consistent with dimer coverings is therefore  $2^{N/6-(L-1)}$ . Since each of these configurations is associated with  $2^L$  dimer coverings, the total number of dimer coverings is

$$\mathcal{Z} = 2^{N/6-(L-1)} \cdot 2^L = 2^{N/6+1} \quad (\text{A4})$$

in agreement with Eq. (18).

## APPENDIX B: DETAILS FOR SEC. XI

### 1. Derivation of Eqs. (55)-(56)

Consider an Ising lattice I composed of  $N_I^{(q)}$  sites of degree  $q$ , where  $q$  runs over the positive integers. The total number of sites and bonds in this lattice are, respectively,

$$N_I = \sum_{q \geq 1} N_I^{(q)}, \quad (\text{B1})$$

$$N_{I,b} = \frac{1}{2} \sum_{q \geq 1} q N_I^{(q)}. \quad (\text{B2})$$

Fisher<sup>10</sup> introduces an “expanded” lattice E in which each vertex of degree  $q \geq 4$  in I is replaced by a “cee” of  $q-2$  vertices of degree 3 and  $q-3$  additional bonds connecting these. Thus the number of sites and bonds in E are, respectively,

$$N_E = \sum_{q=1}^3 N_I^{(q)} + \sum_{q \geq 4} (q-2) N_I^{(q)}, \quad (\text{B3})$$

$$N_{E,b} = N_{I,b} + \sum_{q \geq 4} (q-3) N_I^{(q)} = \frac{1}{2} \sum_{q=1}^3 q N_I^{(q)} + \sum_{q \geq 4} (q-3) N_I^{(q)}, \quad (\text{B4})$$

where in the last expression  $N_E^{(1)} = N_I^{(1)}$ ,  $N_E^{(2)} = N_I^{(2)}$ , and  $N_E^{(3)} = N_I^{(3)} + \sum_{q \geq 4} (q-2) N_I^{(q)}$  (by construction,  $N_E^{(q)} = 0$  for  $q \geq 4$ ).

Next, Fisher introduces a “terminal” lattice, which we will call the Fisher lattice F. It is obtained from E by leaving sites of degree 1 as they are, replacing each site of degree 2 by a pair of new sites (connected by an additional bond), and replacing each site of degree 3 by a triplet of new sites (connected by a triangle of additional bonds). The number of sites in F is therefore

$$N_F = N_E^{(1)} + 2N_E^{(2)} + 3N_E^{(3)} = 2N_{I,b} + \sum_{q \geq 4} (2q-6) N_I^{(q)}. \quad (\text{B5})$$

Furthermore, the number of bonds in F is

$$N_{F,b} = N_{E,b} + N_E^{(2)} + 3N_E^{(3)} \quad (\text{B6})$$

since each site of degree 2 in E gives one new bond and each site of degree 3 in E gives 3 new bonds (the triangle bonds). The number of triangles in F is

$$N_T = N_E^{(3)} = N_I^{(3)} + \sum_{q \geq 4} (q-2) N_I^{(q)} \quad (\text{B7})$$

The number of linking bonds in F is the sum of the first two terms in  $N_{F,b}$ , i.e.

$$N_l = N_{E,b} + N_E^{(2)} = N_{I,b} + \sum_{q \geq 4} (q-3) N_I^{(q)} + N_I^{(2)}. \quad (\text{B8})$$

Eqs. (55) and (56) now follow from these expressions and the fact that  $N_F^{(1)} = N_I^{(1)}$  and  $N_F^{(2)} = 2N_I^{(2)}$ .

### 2. Check of Eq. (57) for Fisher lattices with sites of degree 1 and/or 2

As a check of Eq. (57) when  $N_F^{(1)}$  and/or  $N_F^{(2)}$  are nonzero, let us consider an Ising model in one dimension. First consider the case of periodic boundary conditions. All sites in the Ising lattice I are then of degree 2. The expanded lattice E is therefore identical to I. Continuing to the Fisher lattice F, each site in E is replaced by 2 sites in F. Thus F is simply a 1D chain with an even number of sites with periodic boundary conditions. Obviously, 2 dimer coverings are possible on F in this case, and this indeed also follows from Eq. (57) when we insert  $N_F = N_F^{(2)}$  and  $N_F^{(1)} = 0$ .

Next, consider a 1D Ising lattice with open boundary conditions. Now the two end sites in I have degree 1 while all others have degree 2 as before. Again E is identical to I, while F has twice as many degree-2 sites (so the total number of sites in F is even). Obviously, only 1 dimer covering is possible on F in this case, and this is also what Eq. (57) gives upon inserting  $N_F = N_F^{(1)} + N_F^{(2)}$  and  $N_F^{(1)} = 2$ .

- <sup>1</sup> P. W. Kasteleyn, in *Graph Theory and Theoretical Physics*, ed. F. Harvey (Academic Press, 1967).
- <sup>2</sup> P. Fendley, R. Moessner, and S. L. Sondhi, Phys. Rev. B **66**, 214513 (2002).
- <sup>3</sup> F. Y. Wu, Int. J. Mod. Phys. B **20**, 5357 (2006).
- <sup>4</sup> R. Dijkgraaf, D. Orlando, and S. Reffert, arXiv:0705.1645.
- <sup>5</sup> There is also a considerable mathematical literature on problems involving classical dimers; see e.g. J. Propp, math/9904150; R. Kenyon, math/0310326.
- <sup>6</sup> P. W. Kasteleyn, Physica **27**, 1209 (1961).
- <sup>7</sup> H. N. V. Temperley and M. E. Fisher, Phil. Mag. **6**, 1061 (1961); M. E. Fisher, Phys. Rev. **124**, 1664 (1961).
- <sup>8</sup> M. E. Fisher and J. Stephenson, Phys. Rev. **132**, 1411 (1963).
- <sup>9</sup> P. W. Kasteleyn, J. Math. Phys. **4**, 287 (1963).
- <sup>10</sup> M. E. Fisher, J. Math. Phys. **7**, 1776 (1966).
- <sup>11</sup> R. Moessner and S. L. Sondhi, Phys. Rev. B **68**, 054405 (2003).
- <sup>12</sup> The star lattice is also known under many other names, including the 3-12 or  $3 \cdot 12^2$  lattice,<sup>3,37</sup> the Fisher lattice,<sup>11,34</sup> the decorated hexagonal<sup>35</sup> or expanded kagome lattice,<sup>30,35</sup> and the triangle-honeycomb lattice.<sup>32,36</sup> The name star lattice, which will be used in this paper, was coined in Ref. 37 and was also used in Refs. 28, 29, 31 and (partly) 30.
- <sup>13</sup> K. S. Raman, E. Fradkin, R. Moessner, S. Papanikolaou, and S. L. Sondhi, arXiv:0809.3050.
- <sup>14</sup> R. Moessner and K. S. Raman, arXiv:0809.3051.
- <sup>15</sup> P. W. Anderson, Mater. Res. Bull. **8**, 153 (1973); P. Fazekas and P. W. Anderson, Phil. Mag. **30**, 423 (1974).
- <sup>16</sup> X.-G. Wen, *Quantum Field Theory of Many-Body Systems* (Oxford University Press, 2004).
- <sup>17</sup> D. S. Rokhsar and S. A. Kivelson, Phys. Rev. Lett. **61**, 2376 (1988).
- <sup>18</sup> R. Moessner and S. L. Sondhi, Phys. Rev. Lett. **86**, 1881 (2001).
- <sup>19</sup> G. Misguich, D. Serban, and V. Pasquier, Phys. Rev. Lett. **89**, 137202 (2002).
- <sup>20</sup> A flippable loop is an even-length loop in which the bonds along the loop alternate between being occupied and unoccupied by a dimer. The “flip” interchanges occupied and unoccupied bonds and is equivalent to shifting the dimers by one bond length along the loop.
- <sup>21</sup> V. Elser and C. Zeng, Phys. Rev. B **48**, 13647 (1993).
- <sup>22</sup> G. Misguich, D. Serban, and V. Pasquier, Phys. Rev. B **67**, 214413 (2003).
- <sup>23</sup> F. Wang and F. Y. Wu, Phys. Rev. E **75**, 040105(R) (2007).
- <sup>24</sup> F. Wang and F. Y. Wu, Physica A **387**, 4157 (2008).
- <sup>25</sup> G. Misguich and C. Lhuillier, *Two-dimensional quantum antiferromagnets*, in *Frustrated spin systems*, edited by H. T. Diep (World Scientific, 2003).
- <sup>26</sup> Y. L. Loh, D.-X. Yao, and E. W. Carlson, arXiv:0803.0742.
- <sup>27</sup> In addition to the star lattice, the Archimedean tilings also include the square, triangular, honeycomb, kagome, and Shastry-Sutherland lattice, as well as five other, less frequently encountered lattices; see e.g. Refs. 28 and 37.
- <sup>28</sup> J. Richter, J. Schulenburg, and A. Honecker, Lect. Notes Phys. **645**, 85 (2004).
- <sup>29</sup> J. Richter, J. Schulenburg, A. Honecker, and D. Schmalz, Phys. Rev. B **70**, 174454 (2004).
- <sup>30</sup> G. Misguich and P. Sindzingre, J. Phys.: Condens. Matter **19**, 145202 (2007).
- <sup>31</sup> Y.-Z. Zheng, M.-L. Tong, W. Xue, W.-X. Zhang, X.-M. Chen, F. Grandjean, and G. J. Long, Angew. Chem. Int. Ed. **46**, 6076 (2007).
- <sup>32</sup> H. Yao and S. A. Kivelson, Phys. Rev. Lett. **99**, 247203 (2007).
- <sup>33</sup> S. Samuel, J. Math. Phys. **21**, 2806 (1980).
- <sup>34</sup> D. A. Huse, W. Krauth, R. Moessner, and S. L. Sondhi, Phys. Rev. Lett. **91**, 167004 (2003).
- <sup>35</sup> D. S. Rokhsar, Phys. Rev. B **42**, 2526 (1990).
- <sup>36</sup> S. Dusuel, K. P. Schmidt, J. Vidal, and R. L. Zaffino, arXiv:0804.4775.
- <sup>37</sup> P. N. Suding and R. M. Ziff, Phys. Rev. E **60**, 275 (1999).
- <sup>38</sup> After this work was completed, we became aware that the existence of an Ising pseudo-spin representation for dimer coverings on the star lattice, and the result (18) for the torus, were mentioned (without elaboration) in Ref. 30. We thank Grégoire Misguich for drawing our attention to the discussion of the star lattice in this paper.
- <sup>39</sup> A loop is topologically trivial (nontrivial) if it can (can not) be shrunk to a point. For example, on a torus, loops that wind around the system in one or more of the two toroidal directions are topologically nontrivial.
- <sup>40</sup> To check that this assignment of pseudo-spins to the dodecagons does not produce any contradictions, one can consider arbitrary closed walks visiting dodecagon sites of the dual lattice. An even number of domain walls must be crossed on any such closed walk as otherwise the sign of  $\sigma^z$  would have changed upon returning to the dodecagon one started from. This requirement is indeed satisfied because all domain walls are topologically trivial loops since the two DCs are by assumption in the same topological sector.<sup>22</sup>
- <sup>41</sup> This generalization can be done by introducing a “path of dodecagons”  $D_i$ ,  $i = 1, \dots, n$  going between the two dodecagons, and using  $\hat{\sigma}^z(D_i)^2 = I$ . For example, if  $D'$  is not a neighbor of  $D$  one can write  $\hat{\sigma}^z(D)\hat{\sigma}^z(D') = (\hat{\sigma}^z(D)\hat{\sigma}^z(D_1))(\hat{\sigma}^z(D_1)\hat{\sigma}^z(D_2)) \dots (\hat{\sigma}^z(D_n)\hat{\sigma}^z(D'))$ . Now each pair involves nearest-neighbor dodecagons, so the previous results can be invoked. The end result is the generalization stated in the text.
- <sup>42</sup> X.-G. Wen and Q. Niu, Phys. Rev. B **41**, 9377 (1990).
- <sup>43</sup> D. Dhar and S. Chandra, Phys. Rev. Lett. **100**, 120602 (2008).
- <sup>44</sup> To see this, choose one of the arrows in a constraint to be the ‘output’ and the other arrow(s) to be the ‘input.’ All inputs are valid and determine, via the constraint, the output. Thus a constraint can be used to eliminate the output spin while not restricting the input spin(s). In contrast, the latter property does not hold for (e.g.) dimers on the square lattice, for which the presence/absence of a dimer on a bond corresponds to a bond spin  $\sigma = \pm 1$ , i.e. each site has a hard-core constraint  $\sum_{i=1}^4 \sigma_i = -2$ . Here an input in which more than one of the three input spins is +1 is not valid. Thus the constraint not only determines the output but also puts restrictions on the input. This is consistent with the number of dimer coverings which is asymptotically  $2^{NG/(\pi \ln 2)} \approx 2^{0.42N}$ , since writing this as  $2^{\mathcal{N}_a - \mathcal{N}_e}$  where  $\mathcal{N}_a = 2N$  is the number of spins and  $\mathcal{N}_e$  is the number of eliminated spins due to the constraints, we get  $\mathcal{N}_e \approx 1.58N$ , i.e. each constraint effectively eliminates

1.58 > 1 Ising variables.

<sup>45</sup> Note that the intensive entropy  $(1/3) \log 2$  quoted for the star lattice in Ref. 3 is the entropy per dimer, not per lattice site.

<sup>46</sup> More generally, the magnitude of  $A_{ij}$  is set equal to the (nonnegative) weight of the dimer that can occupy bond  $ij$ ; different bonds can be assigned different weights. In this paper we will only be concerned with the case when all dimers have the same weight, which can then be set equal to 1.

<sup>47</sup> These fixed bond arrows (which we will sometimes refer to as Kasteleyn arrows) should not be confused with the arrows introduced in Sec. II, which are dynamical degrees of freedom living on the lattice sites.

<sup>48</sup> See Ref. 1 for a detailed discussion.

<sup>49</sup> F. Y. Wu and F. Wang, *Physica A* **387**, 4148 (2008).

<sup>50</sup> A. Ioselevich, D. A. Ivanov, and M. V. Feigelman, *Phys. Rev. B* **66**, 174405 (2002).

<sup>51</sup> If the dimer weights are not all equal to 1, the fermionic correlation function on the right-hand side will be multiplied by a weight-dependent prefactor; see Ref. 24.

<sup>52</sup> This also includes the case when the two non-overlapping imprints are part of the same triangle, by each containing an arrow of the triangle. Then the direction of the arrow on the third site of the triangle also becomes fixed, and in turn the arrow on the other side of its linking bond. Furthermore, the triangle constraint and the linking bond constraint are spent. Thus in this case there are further

contributions to  $\Delta\mathcal{N}_a$  and  $\Delta\mathcal{N}_c$  in addition to those from the individual dimer imprints. However, since the numbers of additional spent arrows and constraints are equal, they cancel in  $\Delta\mathcal{N}_a - \Delta\mathcal{N}_c$ .

<sup>53</sup> G. Misguich and F. Mila, *Phys. Rev. B* **77**, 134421 (2008).

<sup>54</sup> For the system with monomers, the “normal” sites (i.e. those that are not occupied by a monomer) should be touched by exactly one dimer as usual. Only the case with an even number of monomer sites is nontrivial; for the odd case no dimer coverings are possible.

<sup>55</sup> A cut point is a site that, if removed, would make the graph disconnected.

<sup>56</sup> J. O. Fjærestad (unpublished).

<sup>57</sup> Note that the triangle that site  $i$  belonged to (before the bonds connected to  $i$  were removed) is replaced by the single bond connecting the two remaining sites of the original triangle. There is then an arrow constraint on this bond which is the same as for a linking bond, i.e. both in or both out. Thus the original triangle constraint has been replaced by a linking bond constraint, giving a net contribution of 0 to  $\Delta\mathcal{N}_c$  from this process.

<sup>58</sup> A. J. Phares and F. J. Wunderlich, *Nuovo Cimento Soc. Ital. Fis.* **101B**, 653 (1988); V. Elser, *Phys. Rev. Lett.* **62**, 2405 (1989).

<sup>59</sup> R. Siddharthan and A. Georges, *Phys. Rev. B* **65**, 014417 (2001).